Click chemistry for block polysaccharides with dihydrazide and dioxyamine linkers - a review

Amalie Solberg,[a] Ingrid V. Mo,[a] Line Aa. Omtvedt,[a] Berit L. Strand,[a] Finn L. Aachmann,[a] Christophe Schatz,*[b] and Bjørn E. Christensen*[a]

[a] NOBIPOL, Department of Biotechnology and Food Science, NTNU Norwegian University of Science and Technology, Sem Sælands vei 6/8, NO-7491 Trondheim, Norway
[b] LCPO, Université de Bordeaux, UMR 5629, ENSCBP, 16, Avenue Pey Berland, 33607 Pessac Cedex, France

Engineered block polysaccharides is a relatively new class of biomacromolecules consisting of chemical assembly of separate block structures at the chain termini. In contrast to conventional, laterally substituted polysaccharide derivatives, the block arrangement allows for much higher preservation of inherent chain properties such as biodegradability and stimuli-responsive self-assembly, while at the same time inducing new macromolecular properties. Abundant, carbon neutral, and even recalcitrant biomass is an excellent source of blocks, opening for numerous new uses of biomass for a wide range of novel biomaterials. Among a limited range of methodologies available for block conjugation, bifunctional linkers allowing for oxyamine and hydrazide 'click' reactions have recently proven useful additions to the repertoire. This article focuses the chemistry and kinetics of these reactions. It also presents some new data with the aim to provide useful protocols and methods for general use towards new block polysaccharides.

1. Introduction

Abundant biomass is basis for extensive industrial production of many polysaccharides. They are widely used as food additives or as pharmaceutical formulations (Draget, Moe, Skjåk-Bræk, & Smidsrød, 2006). They may also have specific, structure-dependent biological effects such as stimulating the immune system (Espevik, Rokstad, Kulseng, Strand, & Skjåk-Bræk, 2009; Suzuki, Christensen, & Kitamura, 2011). As a move towards a new and fundamentally different generation of functional polysaccharides scientists have initiated research on engineering block polysaccharides which consist of at least two polysaccharide blocks covalently linked through their chain ends. This involves first excising relevant blocks, normally oligosaccharides, from parent polysaccharides by standard chemical or enzymatic methods, followed by re-conjugation at the chain termini to form new and well-defined macromolecular architectures. This concept is partly inspired by synthetic or semisynthetic block copolymers but differs by being based entirely on modules obtained directly from biomass (Fig. 1).

Only a limited number of suitable block coupling methods have been described in the literature. In this review we focus on the recent application of oxyamine and hydrazide 'click' reactions for coupling oligo-and polysaccharide blocks terminally. Dihydrazide and dioxyamine molecules have been specifically selected to achieve rapid and quasi-quantitative coupling of polysaccharides through their chain ends, mostly the reducing end but also the non-reducing end after its proper activation. Coupling with these difunctional molecules has several advantages over the more conventional approach based on the

Huisgen azide-alkyne cycloaddition. It includes the absence of copper catalyst which could cause polysaccharide degradation and interaction with some anionic polysaccharides (alginate, pectin, hyaluronan). It also provides a simple two-step coupling pathway: First the activation of one block with a dioxyamine or a dihydrazide followed by the coupling to the second block based on the same chemistry.
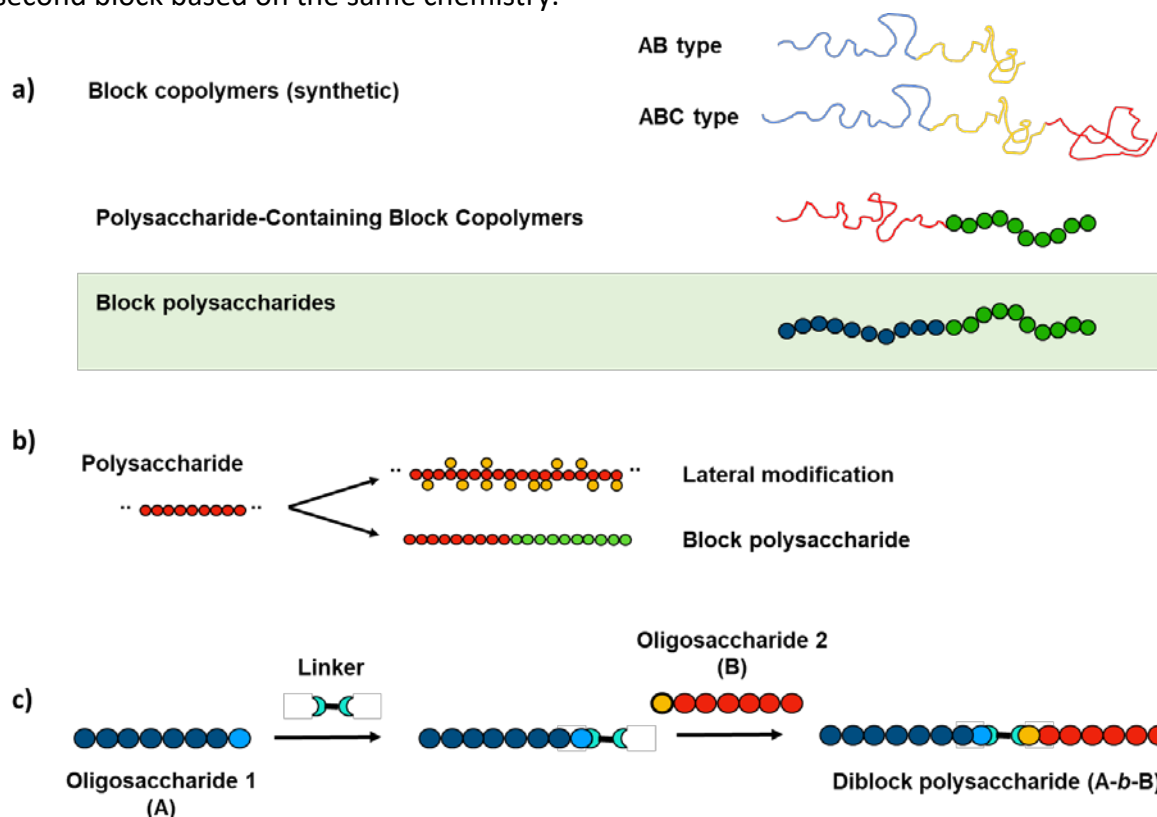

Fig. 1. a) The principal types of engineered block polymers. b) Comparison between polysaccharide derivatives and block polysaccharides. In the latter the chains remain laterally unsubstituted, exposing the chains for interactions otherwise prevented in laterally substituted polysaccharides. c) General strategy for preparing A-*b*-B diblock polysaccharides by first activating the reducing end of one block with a divalent linker before coupling to the reducing end of a second block. Note that the same chemistry is involved in each step.

2. Terminal versus lateral conjugation

Laterally substituted polysaccharides are generally referred to as polysaccharide derivatives. Among the industrially produced derivatives the cellulose derivatives stand out, not only in terms of annual industrial production, but also by affecting inherent physical properties of cellulose chains associated with insolubility and crystallinity (Oprea & Voicu, 2020). Instead, cellulose derivatives are mostly water-soluble (e.g. carboxymethyl cellulose (CMC or hydroxyethyl cellulose (HEC)) and have very different properties and applications than cellulose, including micro- and nanocrystalline cellulose. Others cellulose derivatives such as methyl cellulose (MC) and hydroxypropyl cellulose (HPMC) may self-assemble upon heating due to their lower critical solution temperature (LCST) properties, but here the self-association is governed by hydrophobic substituents and not by reverting to the original chain-chain interactions of cellulose.

Terminal substitutions of polysaccharides are (by definition) restricted to the reducing ends (REs) and the non-reducing ends, respectively, directly giving rise to block structures and architectures. A key feature is that each block in such cases to a large degree retains its inherent properties, in contrast to polysaccharide derivatives having lateral substitutions or modifications masking or suppressing many of the original chain properties (Fig.1b) (Moussa, Crepet, Ladaviere, & Trombotto, 2019; Novoa-Carballal & Muller, 2012). Chain-chain interactions and enzymatic degradation are both favoured by long unsubstituted blocks. The former reflects the cooperative nature of the interactions, often associated with the minimal number of consecutive residues (minimum degree of polymerization, DP_{min}) needed for stable inter chain interactions (Bowman et al., 2016). The latter reflects the steric and chemical requirements of an enzyme (e.g. a hydrolase, lyase, epimerase) to effectively bind to - and cleave - the part of the chain serving as substrate (Christensen & Smidsrød, 1996). Finally, underivatized lateral structures may preserve their biological effects such as interaction with specific receptors.

3. Self-assembly: Lessons from the synthetic polymer field

Block copolymers is a concept originating from the synthetic polymer chemistry field, referring to linear polymers containing distinct blocks of different chemistries (Fig. 1). Conventional block copolymers are widely studied due to their ability to self-assemble into a variety of nanostructures (Fig. 2) as a basis for new materials (Jo, Lee, Zhu, Shim, & Yi, 2017; Lobling et al., 2016; Mai & Eisenberg, 2012). Block copolymers have several useful applications (Schacher, Rupar, & Manners, 2012) such as polymer blend compatibilizers (Ruzette & Leibler, 2005), non-fouling surface coatings (van Zoelen et al., 2014), ordered thin film templates (Hamley, 2009), and nanoscale drug carriers (Kataoka, Harada, & Nagasaki, 2012). Self-assembly of diblock copolymers (in water) is normally controlled by a hydrophobic block forming micellar cores, and a hydrophilic block forming a corona, a behaviour largely governed by the Flory parameter (χ) (Lobling et al., 2016). The particle geometry ranges from spheres to cylinders to bilayer sheets and vesicles (polymersomes). Triblock ABC terpolymers provide a variety of multicompartment nanostructures with C corona and A/B cores, where the ratio of block lengths N_C/N_A controls the morphology (Lobling et al., 2016). Hence, a solid knowledge base exists for block polymers. They are, however, mostly based on one or several synthetic blocks (Schatz & Lecommandoux, 2010) obtained from non-renewable, often petroleum based, sources, rising a serious sustainability issue.
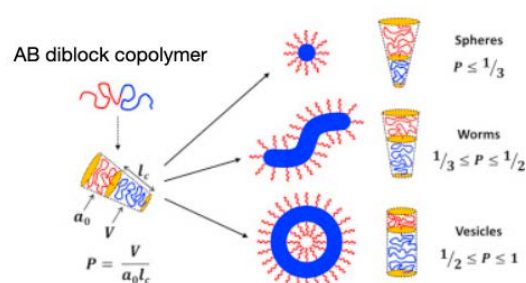

Fig. 2. Illustration of the self-assembly of synthetic or semi-synthetic diblock copolymers: Block parameters governing the assembly modes (*P* is the so-called packing parameter). Reprinted with permission from (Derry, Fielding, & Armes, 2016). Copyright 2021 Elsevier.
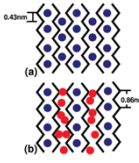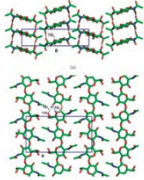
Within the polysaccharide field these concepts are much less developed. Although some polysaccharides such as alginates and pectins may be categorized as block polymers because they consist of identifiable modules or blocks that can be isolated by partial and selective degradation, they still have considerable structural heterogeneity, for example variable distribution and position of blocks within the chains.
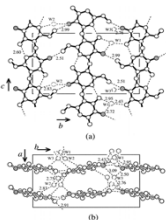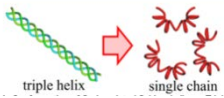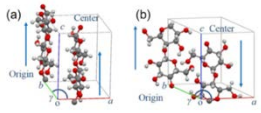
Polysaccharide-containing block copolymers (Fig. 1) represent a first step in incorporating polysaccharides in engineered polymers. In particular, steps have been taken to introduce polysaccharides as the hydrophilic block in self-assembling synthetic block copolymers (Belbekhouche, Ali, Dulong, Picton, & Le Cerf, 2011; Chen, Wah Ng, & Weil, 2020; Daus, Elschner, & Heinze, 2010; Lohmann et al., 2009; Otsuka et al., 2013; Schatz et al., 2010; Upadhyay et al., 2009). Yet, the assembly is still governed by the self-association of the synthetic (hydrophobic) blocks. Non-assembling polysaccharides with PEG-like (polyethylene glycol) properties (uncharged, flexible chains) like dextran and malto-oligosaccharides have typically been used (Schatz et al., 2010). The function of the polysaccharide chain is to form a stable outer interphase (corona) in water.

It should in principle be possible to tailor stimuli-responsive self-assembling block polysaccharides by terminally conjugating a polysaccharide block whose solubility depends on physicochemical conditions coupled to an inert (non-assembling) polysaccharide block. Clearly, the most attractive systems would be those assembling in an aqueous environment by simple stimuli such as ionic strength, specific salts, pH or temperature. Some examples are given subsequent sections, but the field is otherwise remarkably little studied. This is in stark contrast to the abundance of such polysaccharides and the numerous studies of their self-association, for example in the context of gel formation.

4. Polysaccharides: Large variation in solution properties and self-assembly modes

Abundant polysaccharides do indeed have a much wider range of solution and self-assembly properties than often recognised. Although many polysaccharides, especially those of microbial origin, are highly water-soluble and do not self-associate under normal aqueous conditions, others are inherently water-insoluble and even crystalline in the native state like, for example, cellulose or chitin. A third category is polysaccharides that may undergo a disorder-order transition in solution when the conditions are changed (temperature, ionic strength, pH, co-solvents, specific salts, etc). Examples of abundant polysaccharides possessing self-assembly properties, as well as self-assembly modes and stimuli needed to induce self-assembly are shown in Table 1.

Table 1. Chain stiffness and self-assembly characteristics of selected oligo- and polysaccharides. *q = persistence length (nm), a chain stiffness parameter for the solution state

	q*	Self-assembly modes		Self-assembly stimuli
Alginate (Oligoguluronate/G-blocks)	15		Schematic structure of G-rich alginate junction zones. (a) Long-range Ca^{2+}-mediated inter-action between chains. (b) Ca^{2+}-mediated dimers that pack through unspecific interactions. Blue and red spheres represent site-bound and non-site bound Ca^{2+} ions, respectively. Reprinted with permission from (Sikorski, Mo, Skjåk-Bræk, & Stokke, 2007). Copyright 2021 American Chemical Society.	Selective cations: Ca^{++}, Ba^{++}, Sr^{++} Carboxylate protonation (pH < pK_a).
Chitin	6-8		Views perpendicular to the *ab*- (a) and *bc*- (b) planes of the α-chitin structure. Reprinted with permission from ((Sikorski, Hori, & Wada, 2009). Copyright 2021 American Chemical Society.	Solvent change (e.g. DMAc to water). Temperature change: Phase separation in alkaline conditions with a lower critical solution temperature (LCST)

Chitosan			Packing structure of hydrated chitosan projected along the *a*-axis (a) and along the *c*-axis (b). Filled circles denote nitrogen atoms. For the sake of clarity, only three polymer chains of the lower layer in (b) are shown in (a). Reprinted with permission from (Okuyama, Noguchi, Miyazawa, Yui, & Ogawa, 1997). Copyright 2021 American Chemical Society.	Amine deprotonation (pH > pK_a) Selective ions: triphosphate, citrate, Cu^{++}, Zn^{++}. Complexation at pH < pK_a with polyanions. Gelation at high concentration (> C*) in alkaline conditions LCST behaviour at pH > pK_A in presence of glycerol phosphate.
β-1,3 glucans	3.5		Triple-helix of β-1,3-glucans. Reprinted with permission from (Tomofuji, Yoshiba, Christensen, & Terao, 2019). Copyright 2021 Elsevier.	Solvent change (DMSO). Neutralisation from high pH.
Cellulose	8		The unit cells of cellulose Iβ (a) and cellulose II (b) crystals. Adapted with permission from (Hayakawa, Nishiyama, Mazeau, & Ueda, 2017). Copyright 2021 Elsevier.	Solvent change (e.g. DMAc/LiCl to water).

Alginates are industrially utilised polysaccharides isolated from brown seaweeds with rather unique self-assembling properties. Alginate may also be produced by several bacterial strains. Despite being unbranched and having only two different monomers, 4-linked-b-D-mannuronate (M) and its 5-epimer 4-linked a-L-guluronate (G), the latter being introduced at the polymer level by mannuronan-C5 epimerases, natural alginates have a heterogeneous block structure whose arrangement is not known in all details. Alginates containing G-blocks tend to form hydrogels in the presence of calcium ions. This self-assembly is associated with the formation of interchain junctions between G-blocks, which due to the 'cavities' formed by the $^1C_4$ conformation of the G residues bind calcium strongly, in contrast to M-blocks and alternating (..MGMG..) blocks (Donati & Paoletti, 2009). The junction zones are often referred to as the 'egg box model' (Table 1, top). By incorporating purified G-blocks in diblock polysaccharides containing a calcium-insensitive, hydrophilic dextran as the second block, calcium-induced self-assembly leading to nanoparticles was obtained (see below).

Chitin forms an integral part of exoskeletons of crustaceans and insects. Once purified they appear as water-insoluble, crystalline materials, as illustrated in Table 1. Chitins dissolve in solvents like DMAc-LiCl or in strong alkali below a critical lower solution temperature (LCST) (Goycoolea et al., 2007). Recrystallisation upon transfer back to water is a form of self-assembly that so far (in the present context) has been little studied.

Self-assembly of most chitosans, the exception being short oligomers and chitosans with a residual fraction of N-acetylated residues in the range 0.4-0.6, occurs when pH is risen above the pK_a (ca. 6.5) and the chains consequently lose their polyelectrolyte character. Increase of pH is therefore a convenient stimulus to induce self-assembly, but also complexation with selective ions like triphosphate, citrate, Cu^{++}, Zn^{++} or polyelectrolytes like DNA, hyaluronan or albumin may be applied (Guibal, Touraud, & Roussy, 2005; Wu et al., 2020). It has also been shown that chitosan solutions can form gels without addition of crosslinkers, either by starting from a hydroalcoholic solution after water evaporation (Montembault, Viton, & Domard, 2005a) or from simple chitosan solution with DA < 30% in presence of ammonia

vapour (Montembault, Viton, & Domard, 2005b). In both cases, the chitosan concentration must be above the critical C* where interaction or overlapping of polymer chains occurs.

b-1,3-linked glucans such as scleroglucan and schizophyllan (and others) form rigid but water-soluble triple helical structures. They can disintegrate into semiflexible coils either at high pH or in special solvents such as DMAC/LiCl. Return to aqueous conditions partially restores triple-helical sequences but the overall morphology for high molecular weights includes aggregates, circular species, and triple helixes (Sletmoen & Stokke, 2008).

The situation for cellulose resembles that of chitin. They occur naturally as partly crystalline forms (Cellulose I). When regenerated from cellulose solvents they can form another crystal form (Cellulose II) (Sjöström, 1993).

5. Conjugation at the reducing end.

The reducing end is the primary target for preparing diblock polysaccharides. Irrespective of the method used all conjugations involves at least activation of one of the blocks before conjugation to the second. The reducing end position of oligo- and polysaccharides, which in most cases involves an aldose, consists of a small proportion of free aldehyde in equilibrium with the dominating hemiacetal form. Hence, the first step in all current conjugation processes is a reaction of the aldehyde with an amine to form a Schiff base (imine). In most cases the Schiff base is then selectively reduced to obtain a stable bond (see 5.2.2).

5.1. Alkyne-azide Huisgen cycloaddition (Cu dependent or Cu free)

Alkyne-azide Huisgen cycloaddition is a widespread method to conjugate two separate molecules and forms an integral part of bioorthogonal chemistry (Bertozzi, 2011; Sletten & Bertozzi, 2009). It is, however, a multistep approach when conjugating two carbohydrate chains since both chains first need to be reacted separately with an alkyne amine and an aminoazide, respectively, as demonstrated in the formation of a dextran-based diblock polysaccharide (Fig. 3).
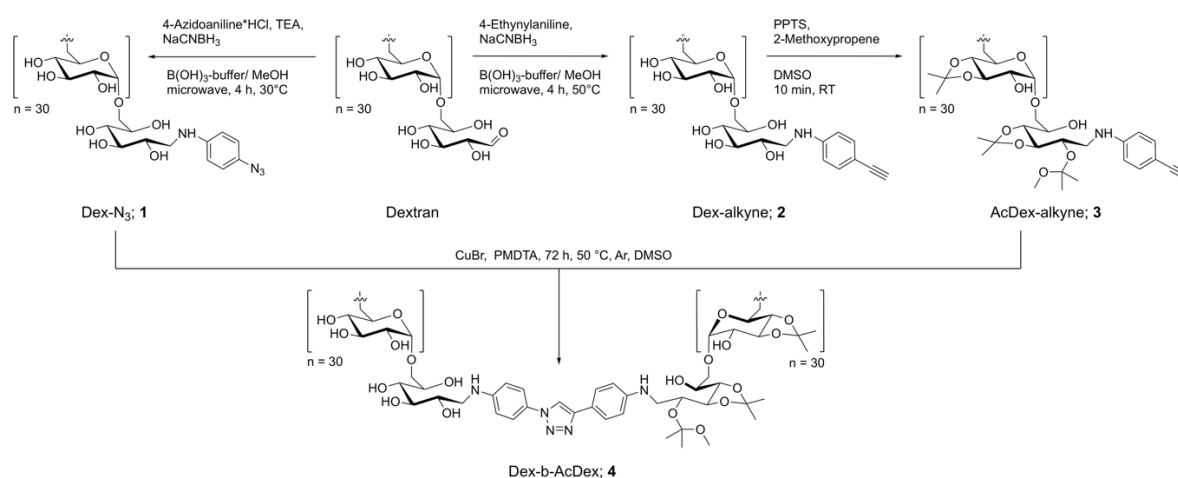

Fig. 3. Synthetic Route to the Amphiphilic Dex-*b*-AcDex Block Copolymer (4) by Cu(I)-Mediated Click Reaction of a Hydrophilic Azide-Functionalized Dextran Block (1) with a Hydrophobic Alkyne-Functionalized Acetalated Dextran Block (3). Reprinted with permission from (Breitenbach, Schmid, & Wich, 2017). Copyright 2021 American Chemical Society.

The major advantage of this methodology is the fast and highly selective (orthogonal) cycloaddition step requiring only equimolar proportions of reacting chains. The cycloaddition itself can be of two types. The Cu-dependent reaction shown above is by far the most common for other types of polysaccharide conjugates. For charged polysaccharides such as alginates this method becomes challenging due to the strong binding of copper ions (Haug & Smidsrød, 1965) (also see below). Depolymerisation can further become significant because the copper ions may catalyse free radical induced reactions (Fenton type), eventually leading to chain scission (Lallana, Fernandez-Megia, & Riguera, 2009). The approach was recently explored to prepare β- and γ-cyclodextrin-end-substituted alginate (alginate-CD diblock). The alginate reducing end was first reacted with alkyne hydrazide using the hydrazide click chemistry previously described for chitin (Mo, Feng, et al., 2020), chitosan and dextran (Mo, Dalheim, Aachmann, Schatz, & Christensen, 2020), and alginate (Solberg, Mo, Aachmann, Schatz, & Christensen, 2021). Following hydrazide conjugation subsequent Cu-mediated click reaction carried out with azide-substituted β- and γ-cyclodextrin in 40% DMSO containing 0.3 mM $CuSO_4$ (50°C, 5 days) seemed to work with M and MG oligomers. However, testing these reaction conditions with G-oligomer the copper-based click-chemistry failed (see Supplementary Information file, S4). This finding confirms that Cu-mediated click chemistry is not always applicable to prepare alginate based diblocks. However, this may be avoided by applying copper free click chemistry. In this case the alginate chains were first terminally activated with azide-substituted oxyamine-PEG using an oxime click protocol developed for alginate (Solberg et al., 2021). Subsequent click reactions with either a dibenzocyclooctyne (DBCO) substituted peptide or a DBCO substituted fluorescent probe (Alexa) proceeded effectively. Data are provided in the Supplementary Information file.

It should be noted that other methods for conjugation at the reducing end of carbohydrates exist. These include thioacetylation (Pickenhahn et al., 2015) and thiol-ene chemistry (Heise et al., 2021; Mergy, Fournier, Hachet, & Auzely-Velty, 2012).

5.2. The oxyamine and hydrazide click chemistry

5.2.1. Chemistry and conjugation order

The main motivation for introducing oximes and hydrazide click reactions is that they react relatively fast with reducing carbohydrates, in contrast to most primary amines (Kwase, Cochran, & Nitz, 2013). This is due to the higher nucleophilicity of oxyamine and hydrazide groups which arises from the so-called alpha effect, that is, the increase in the HOMO energy due to the overlap of orbitals of neighbouring (alpha) atoms having lone electron pairs (Edwards & Pearson, 1962). In addition, the weak basicity of oxyamine and hydrazide (pK_a < 4-5) allows to use them in slightly acidic conditions, which is particularly relevant for systems like chitosans, that are not soluble at neutral pH. These chemistries may be particularly useful in systems where conventional Cu-based click chemistry does not function properly but have been shown to work well with a range of oligo- and polysaccharides as recently demonstrated in our laboratory using dioxyamines and dihydrazides to produce diblock polysaccharides (Mo, Dalheim, et al., 2020; Mo, Feng, et al., 2020; Solberg et al., 2021).

For preparing a A-*b*-B diblock polysaccharides the general strategy is to first react (activate) one of the blocks with a dioxyamine such as O,O'-1,3-propanediyl-bishydroxylamine (PDHA) or a dihydrazide such as adipic acid dihydrazide (ADH) (Fig. 4a). Both the first and the second conjugation involves the same type of chemistry. Which block to choose for the first conjugation (block A) depends on many factors, including the relative reactivities, concentrations and subsequent purifications to remove the reagent in excess (Mo, Dalheim, et al., 2020; Mo, Feng, et al., 2020; Solberg et al., 2021).

The primary reaction products (Figure 4b) are in both cases acyclic E- and Z- hydrazone or oxime isomers, which both can react further to give N-pyranosides and N-furanosides (Baudendistel, Wieland, Schmidt, & Wittmann, 2016; Kwase et al., 2013). Especially hydrazides are prone to convert to N-pyranosides with normal reducing ends (Table 2), whereas in the special case of 2,5-anhydro-D-mannose (M unit) (nitrous acid degraded chitosan) cyclic forms cannot form (Mo, Dalheim, et al., 2020).
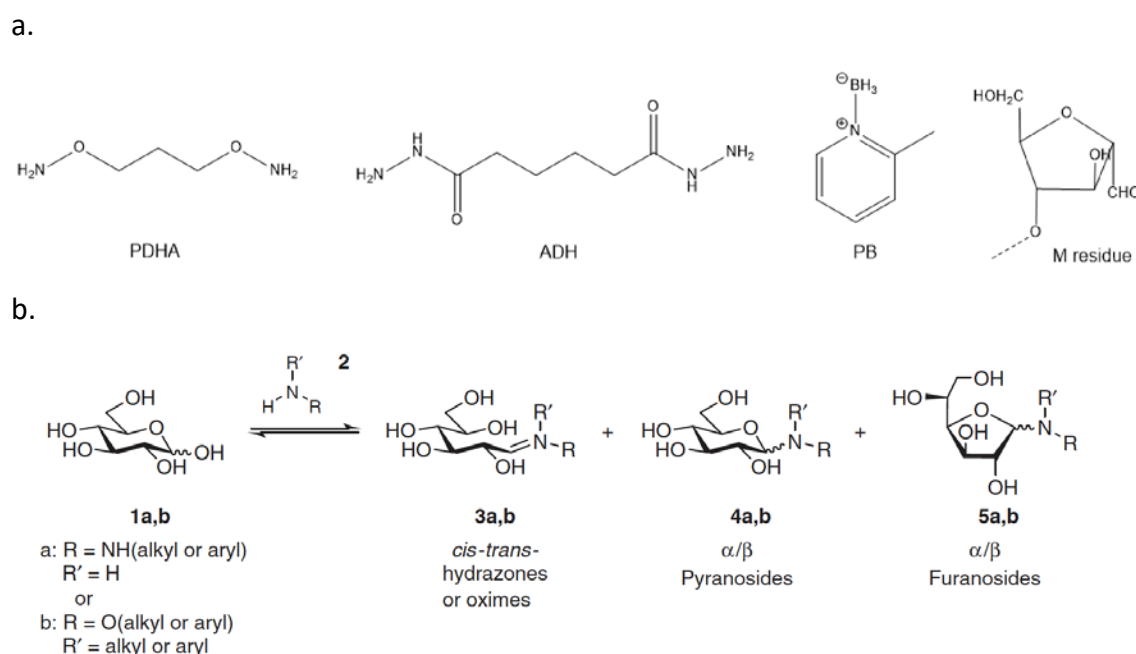
a.

b.

Fig. 4. a) Structure of bifunctional linkers PDHA and ADH, the reducing agent α-picoline borane (PB) and the 2,5-anhydro-D-mannose (M unit) reducing end of nitrous acid degraded chitosans. b) Tautomeric equilibrium with hydrazide and oxyamine glucosyl condensation products. Reprinted with permission from (Kwase et al., 2013). Copyright 2021 Wiley & Co.

Table 2: The distribution of conjugates (acyclic: cyclic) at equilibrium obtained when conjugating polysaccharides and oxyamines or hydrazides (500 mM acetic acid buffer, pH 4 at 22°C). Acyclic refers to E/Z hydrazones (with ADH) or E/Z oximes (with PDHA) while cyclic corresponds N-pyranosides and N-furanosides. For chitosan, D refers to D-glucosamine and A refers to N-acetyl D-glucosamine. X can be either A or D.

Polysaccharide		Ratio acyclic: cyclic	
	Reducing end	PDHA	ADH
Dextran	6-linked D-glucose	4.3:1	1:41

| β-1,3-glucan	3-linked D-glucose	5.1:1	1:44
Chitosan (D_nXA type)	4-linked N-acetyl-D-glucosamine	5.4:1	1:1
Chitosan (D_nM type)*	4-linked 2,5-anhydro-D-mannose	1:0	1.0
Chitin (A_nM type)*	4-linked 2,5-anhydro-D-mannose	1:0	1:0
Mannuronan	4-linked D-mannuronic acid	1:0	1:1.2
Guluronan	4-linked L-guluronic acid	1:0	1:27
Galacturonan	4-linked D-galacturonic acid	n.d.	1:6.7
Amylose (or Maltose)	4-linked D-glucose	2.6:1	n.d.
* It is not possible to form cyclic N-pyranosides or N-furanosides with the 2,5-anhydro-D-mannose reducing end			

5.2.2. Oxime and hydrazone reduction

In many cases unreduced oximes and hydrazones may be the targeted end products, but they are normally further reduced to the corresponding secondary amines. This not only stabilises the linkage irreversibly but also simplifies the chemistry to a single secondary amine. Although sodium cyanoborohydride ($NaBH_3CN$) historically has been the most common reductant used for this type of reactions, and generally for classical reductive aminations, the introduction of the non-toxic α-picoline borane (PB) (Cosenza, Navarro, & Stortz, 2011) as an alternative reductant has been investigated and often found to function well when reacting carbohydrates with both oxyamines and hydrazides. In comparative assays with ADH and PDHA conjugates obtained with chitosan carrying a M unit at the reducing end, cyanoborohydride reacted initially 2-3 times faster than PB at pH 4.0 (Mo, Dalheim, et al., 2020), but the latter seemed to disintegrate more slowly although multiple addition are needed to achieve complete reduction. For most carbohydrates the reduction of the reducing end by $NaBH_3CN$ or PB is negligible compared to that of their oximes or hydrazones. However, it may be noted that chitin oligomers obtained by nitrous acid degradation, and presumably all oligosaccharides terminating in M (2,5-anhydro-D-mannose), become rapidly reduced by both sodium cyanoborohydride and PB. This necessitates a two-step protocol involving first the formation of oxime/hydrazone, followed by a subsequent reduction step (Mo, Dalheim, et al., 2020). Interestingly, the reduction with PB is strongly pH dependent, and increases rapidly with decreasing pH (investigated range pH 3-5).

6. Oxime and hydrazide click reactions: Conjugation kinetics and kinetic modelling

Reaction modelling is a useful tool to compare reactivities of ADH and PDHA against various reducing end types, to optimise reaction conditions (pH, T, concentrations), and to compare different reaction protocols, for example choosing which block to activate first, or predicting reaction outcome under conditions where reaction monitoring is not feasible (e.g. dilute solutions and high molar masses). Oxime and hydrazide reactions are often considered to be slower than conventional (Huisgen cycloaddition type) click reactions and will normally

require one of the reactants in excess, which later must be removed during purification. For block polysaccharides it is further particularly important to determine the influence of the DP. Short chains are ideal for studying reaction kinetics by NMR, but this becomes progressively more difficult with long chains when resonances from the linker regions become relative weaker compared to the general signal intensities. Moreover, viscosity issues often appear for long chains, necessitating dilution, which lowers the reaction rates in addition to broadening NMR resonances. Hence, extrapolation of reaction rates from more concentrated system with low DP may be necessary to predict and decide on optimal protocols (Solberg et al., 2021).One should also bear in mind that the coupling between polysaccharides blocks of rather high DP (> 100) is difficult to achieve due to low probability of chain-end encountering whatever the type of coupling chemistry being involved.
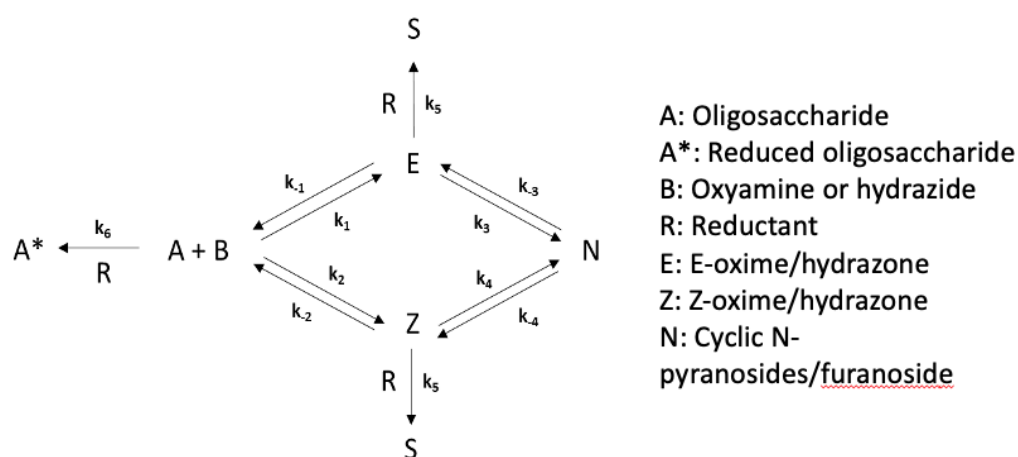
Scheme. 1. General reaction scheme for the reaction of an oligosaccharide (A) with an oxyamine or hydrazide (B) in the presence of a reducing agent (R). Rate constants used in reaction modelling are included. It is assumed that the oxime/hydrazone and oligosaccharide reductions are irreversible. It is further assumed that E- and Z-oximes/hydrazones are reduced at the same rate, and that N-pyranosides can be treated as a single component. Note that in the case of 2,5-anhydro-D-mannose no cyclic forms can be formed ($k_3 = k_{-3} = k_4 = k_{-4} = 0$). Adapted from (Mo, Dalheim, et al., 2020).

6.1. Kinetics of oxime and hydrazone formation

For simple modelling and comparison of carbohydrate-oxyamine reactions a purely empirical model to fit experimental data has been developed for oximes (Baudendistel et al., 2016). The model yields the times to reach 50% ($t_{0.5}$) and 90% ($t_{0.9}$) of the oxime equilibrium values, treating the E- and Z-oximes and the cyclic N-pyranosides/furanosides as a single (combined) reaction product. Such empiric parameters permit direct comparison of different reactants, for example different carbohydrates or different oxyamines, provided data were obtained at identical concentrations of reactants. However, modelling the effect of changing concentrations requires a different approach. Hence, as a step towards a more generally applicable model we therefore investigated a range of reactions by applying a kinetic model (Mo, Dalheim, et al., 2020; Mo, Feng, et al., 2020) based on the Scheme 1 i.e. by assigning individual rate constants for all forward and reverse reactions. The reactions of polysaccharides with free ADH or PDHA (for the first activation), as well as the second reaction (where ADH- or PDHA-activated chains are coupled to a second polysaccharide), were modelled based on first order kinetics with respect to the concentrations of each

reactant. Hence, using the symbols of Scheme 1, the model is based on the equations of the following type:

$$\frac{d[A]}{dt} = -k_1[A][B] + k_{-1}[E] - k_2[A][B] + k_{-2}[Z] - k_6[A][R]$$
$$\frac{d[E]}{dt} = -k_1[A][B] + k_{-1}[E] - k_3[E] + k_{-3}[N] - k_5[E][R]$$
$$etc..$$

The complete set of equations has been published elsewhere (Mo, Dalheim, et al., 2020) (Supporting information file S3 of the reference). Criteria for determining the rate constants included - in addition to minimising the sum of the least squares – the fact that all differentials (d[A]/dt, d[B]/dt, d[E]/dt etc.) approached zero for long reaction times since this was in all cases observed experimentally. It had further to be assumed that k_3 equals k_4 and k_3 equals k_{-3} to reduce the number of variables. The assumptions should as a first approximation be chemically reasonable. As demonstrated in Figure 5, this approach could well fit the experimental data (obtained by NMR) for several systems, providing all necessary rate constants, and demonstrating the wide applicability of the model. Indeed, no systems have so far been studied which do not fit the model reasonably well.

Data include the activation step with PDHA for the chitin dimer AA (Fig. 5a) and a β-1,3-glucan pentamer (Fig. 5b) under otherwise identical conditions. It is clearly seen the glucan reacts faster and gives higher yields with PDHA than the chitin oligomer. Comparing β-1,3-glucan oligomers with dextran oligomers gave almost identical results with PDHA (unpublished data), suggesting the kinetic data can also be assumed for other common hexoses. Uronic acids are clearly very reactive (Fig. 5d) as demonstrated for equimolar amounts of an alginate trimer and PDHA-substituted β-1,3-glucan (nonamer), yielding about 50% in only 5 hours. The figure also shows new data (Gravdahl, 2021) for chitosan oligomers conjugated to a relatively large PDHA-activated dextran (DP 37). Even with only 7 mM of each block the coupling is too fast for obtaining kinetic data with NMR, and the yield is very high (about 63%).

Oxime and hydrazone reactions with carbohydrates are known to depend on pH (Kwase et al., 2013). This was investigated for the reactions of both ADH and PDHA with chitin (Mo, Feng, et al., 2020) and chitosan (Mo, Dalheim, et al., 2020). The reaction yield was highest around pH 3-4, but kinetics was optimal at pH 5, although the pH dependency in both cases was not very large. It may be noted the oxime/hydrazone reduction rate may decrease considerably with increasing pH, precluding pH 5 as a viable alternative. pH 4.0 has therefore been generally used in our laboratory for all types of oligosaccharides.

For all systems investigated so far, the reaction kinetics of PDHA and ADH did not depend very much on whether an oligosaccharide was reacted to the other end, or not. This seems reasonable considering that the number of bonds between the terminal $-NH_2$ groups is high enough to preserve their intrinsic reactivity after activation of one of them. In fact, dextran oligomers seemed even to react somewhat faster with A_nM-ADH and A_nM-PDHA compared to free ADH and PDHA (Mo, Dalheim, et al., 2020).

For comparative purposes an even simpler model could also be successfully applied. Here the reaction was simplified to the type A + B → AB, where A designated the oligomer and B the amine, whereas AB signified the sum of all conjugation forms (E, Z and N-pyranoside). Here only two rate constants (k_T and k_{-T}) governed the reaction, which is considered first order with respect to concentrations:

$$\frac{d[A]}{dt} = \frac{dB}{dt} = -\frac{d[AB]}{dt} = k_T[A][B] - k_{-T}[AB]$$

For practical purposes this simple equation fitted excellently to experimental data and predicted well the effect of changing the concentrations of reactants (Mo, Dalheim, et al., 2020; Mo, Feng, et al., 2020). The model incorporates, in contrast to that of Baudendiestel et al. (2016), the effects of changing the concentrations of reactants.

Both approaches were in some cases tested to very if the model was valid over a wider concentration interval, i.e., if it were first order. Examples for the reaction of a chitin dimer (AA) with two different concentrations of PDHA or ADH are given in Figure 5e-f.
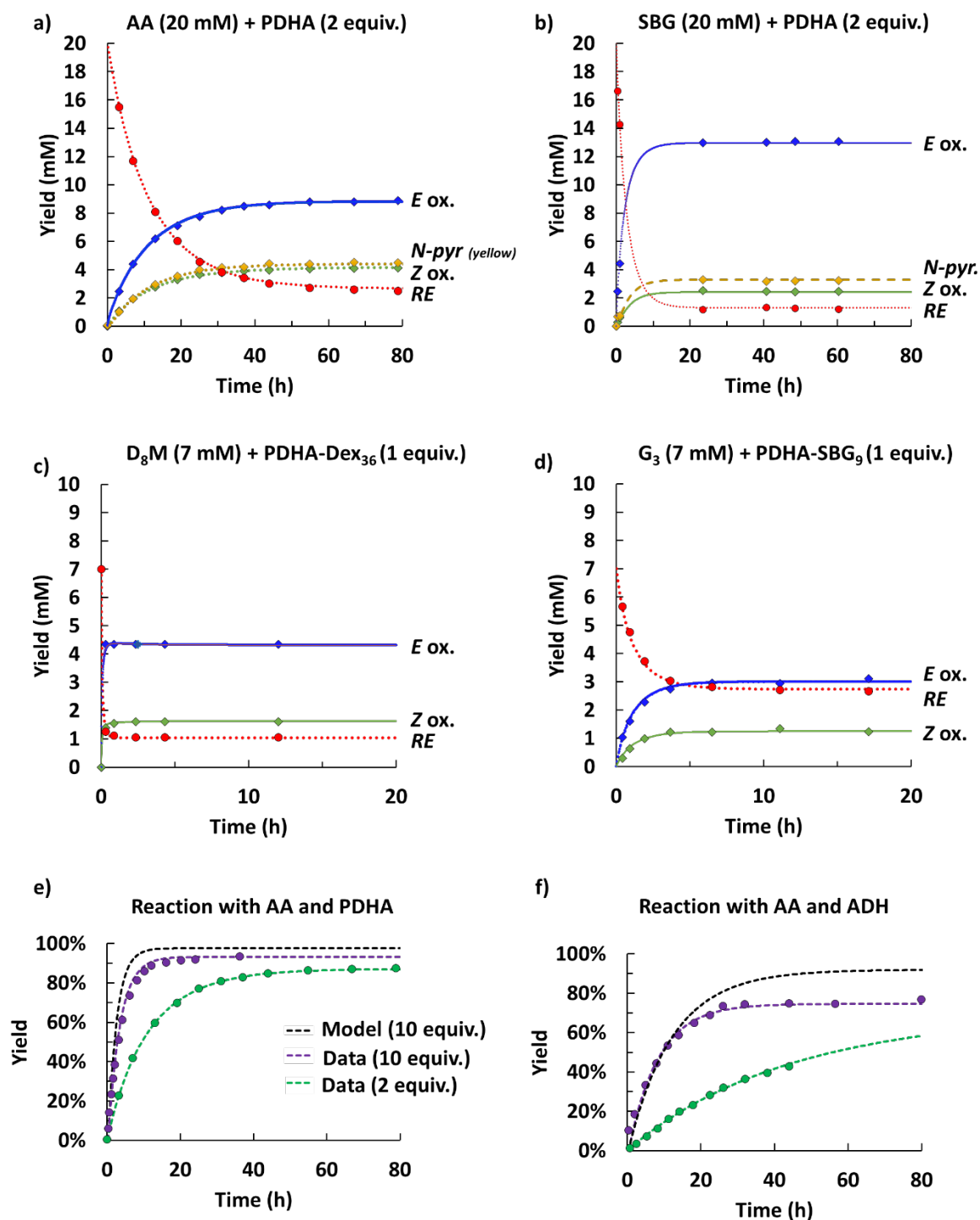
Fig. 5. a-d) Examples of kinetic modelling of experimental data from NMR reaction monitoring using the model described in Scheme 1. e-f) Kinetic modelling of experimental data for the reaction with AA (20 mM) and PDHA or ADH with 2 or 10 equivalents.

Abbreviations: AA: chitobiose (chitin dimer). PDHA: *O,O'*-1,3-propanediylbishydroxylamine. G_3: Oligoguluronate trimer. PDHA-SBG$_9$: PDHA-substituted at the reducing end of a β-1,3-glucan nonamer. SBG$_5$/SBG$_9$ β-1,3-glucan pentamer/nonamer. D$_4$M: Chitosan tetramer with a 2,5-anhydro-D-mannose (M) residue at the reducing end (obtained by chitosan degradation with nitrous acid). Dex$_{36}$-PDHA: PDHA-substituted at the reducing end of a dextran oligomer (SEC fraction) with DP 36. Re: Reducing ends. E ox and Z ox: E and Z oximes. For examples of reactions with ADH, see literature (Mo, Dalheim, et al., 2020; Mo, Feng, et al., 2020; Solberg et al., 2021).

Figure 5e compares data obtained for 20 mM chitobiose (AA) with 2 and 10 equivalents of PDHA. Both data sets can we excellently fitted to the first order models above, but rate constants were not completely identical. Therefore, experimental results for 10 equivalents are slightly below those predicted using the rate constants obtained with 2 equivalents. Although the peak integration in NMR introduces some uncertainty, the data could suggest the reaction, at least in the present case, is not strictly first order. Clearly, more extensive investigations are needed to obtain a more complete picture of the reaction kinetics for a much wider range of concentrations and oligo- or polysaccharides.

The role of DP was investigated with dextran oligomers with DP 1 and 5, respectively, in the reaction with either PDHA or ADH (Mo, Feng, et al., 2020). The results showed marginal differences in the rate constants (k_T and k_{-T}), but possibly slightly faster reaction with PDHA at DP 5. The same trends were observed with chitosans of the type D_nXA, i.e. chains having an N-acetyl D-glucosamine residue (A) at the reducing end, otherwise residues of D-glucosamine (D), except the X position, which can be either A or a D. The chain length was either 5 (n = 2) or 11 (n = 8). Although kinetic data for very large chains have not yet been determined, the results suggests that the kinetic constants are largely independent of the chain length. In total, the two models are particularly useful for predicting the kinetic effects of varying concentrations of reactants. It may be noted that most published data refer to 22°C.

6.2 Kinetics of oxime and hydrazone reduction with α-picoline borane (PB)

When adding an oxime/hydrazone reductant such as PB modelling became much more complex. The reduction step was clearly not first order, and the corresponding rate (k_5 in Scheme 1) did indeed depend on the concentration of reductant. This is partially ascribed to the fact that the PB is partially insoluble in water and sediments during the NMR analyses. It also tends to decompose and needs to be added in portions to obtain complete reduction (Gravdahl, 2021). For the most 'reduction-resistant' systems investigated so far high concentrations of PB combined with high reduction temperature (60°C) provided acceptable reduction rates comparable to aniline- and cyanoborohydride-based protocols (Mo, Feng, et al., 2020).

6.3. Stability and degradation modelling

Whereas reduction of oximes and hydrazones to the corresponding secondary amines yields stable conjugates, the reversibility of the previous steps enables systems that can be tailored for predetermined degradation rates, for example under physiological conditions in the case of biomedical applications. Novoa-Carballal and Müller (2012) demonstrated that a dextran-*b*-PEG oxime became sensitive to acid hydrolysis below pH 3, but relatively stable above.

No experimental stability data are currently available for non-reduced ADH or PDHA-based block polysaccharides, but once the rate constants described above have been determined the degradation process can be modelled. Two examples are given in Figure 6 for the system G_3-PDHA-SBG_9 (oligoguluronate DP3 conjugated to PDHA-activated SBG_9). Rate constants for the forwards (E and Z formation, the amount of N-pyranoside being negligible) and the

reverse reactions were obtained from the data fitting shown in Figure 5d (obtained at pH 4.0). The initial concentrations of E- and Z-oximes were taken to be 10 and 5 mM, respectively, all other concentrations being zero. In a closed system (Fig. 6a) equilibrium is restored after about 4 hours, giving a mixture of remaining G_3-PDHA-SBG$_9$ (6.6 mM) and free G_3 (reducing ends) and PDHA-SBG (both 5.1 mM). In an open system, which would typically meet the conditions expected in various biomedical applications, it is assumed that degradation products are removed, preventing reversal. Hence, all conjugates should become degraded in about 15 hours.
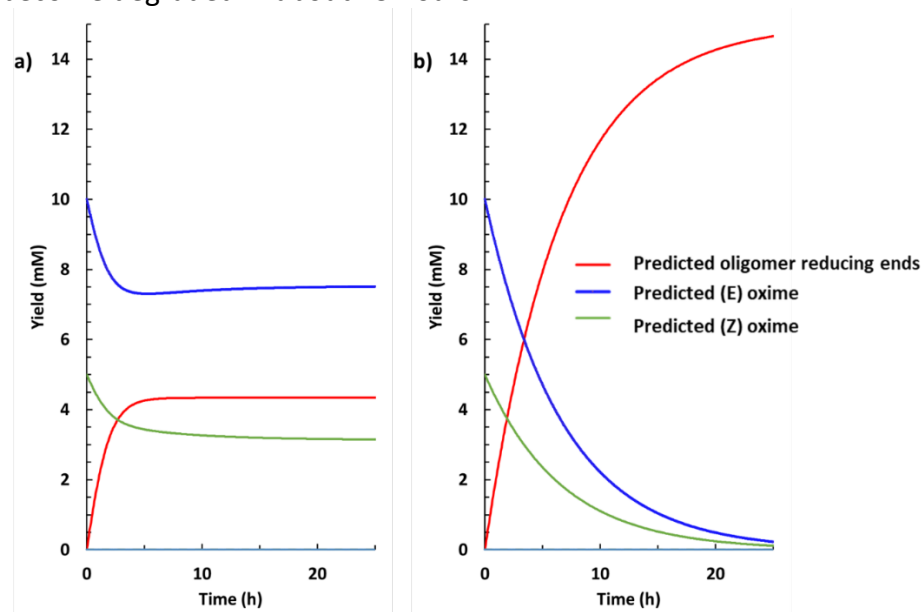

Fig. 6. Simulation of the degradation (at pH 4.0, 22°C) of G_3-PDHA-SBG$_9$ oximes (10 mM E and 5 mM Z, respectively, the oxime linkage being between G_3 and PDHA) based on rate constants derived from Figure 7d. a) Closed system allowing for accumulation of free G_3 and PDHA-SBG$_9$, leading to new equilibrium values. b) Open system where free G_3 and PDHA-SBG$_9$ are continuously removed, preventing reversal.

6.4. Divalent linkers: The double-substitution and ADH polymerisation issues

An aspect with divalent linkers such as PDHA and ADH is that both termini of the linkers may be substituted in the initial activation step. After reaction at one terminus, i.e. after forming a polysaccharide-PDHA conjugate, the reactivity of the remaining free oxyamine (or hydrazide) is high, or sometimes even higher than the free linkers (Mo, Dalheim, et al., 2020; Mo, Feng, et al., 2020). This favours the formation of symmetric diblock polysaccharides with antiparallel chains. Indeed, using 0.5 equivalents of linkers, such diblocks may form in good yields in a single step (Solberg, 2017). Otherwise, for the normal activation step typically 10-20 equivalents of linker should be used to minimise the diblock formation (Mo, Dalheim, et al., 2020).

ADH may pose an additional challenge due to its ability to polymerise under conditions used for polysaccharide conjugation, especially when heated (Mo, Dalheim, et al., 2020; Mo, Feng, et al., 2020). Free ADH indeed forms an insoluble polymer when heated. Also, multiple ADH substitutions could be detected in some cases, although the terminal hydrazide could remain reactive. However, the polymerization kinetics remains rather slow in comparison to amination reactions with ADH.

7. Reactions at the non-reducing ends

The number of methods for selective attachment at the non-reducing ends (NRE) of oligo-saccharides is limited. Chemical methods are restricted to special cases such as limited and selective periodate oxidation (Hirano & Yagi, 1981), which is applicable to e.g. chitin (Fuchs et al., 2018; Imai, Watanabe, Yui, & Sugiyama, 2002). Lyase- or alkali-degraded 4-linked uronides (alginates, hyaluronan, heparin, pectins) having an unsaturated C=C bond between C4 and C5 at the non-reducing end can possibly be substituted by thiol-ene chemistry as recently described for heparin (Wang, Shi, Wu, & Chen, 2014). However, the recent and remarkable development in cellulose- and chitin-degrading lytic monooxygenases (LPMOs) (Horn et al., 2006; Isaksen et al., 2014; Vaaje-Kolstad et al., 2010) provides a new class of oligosaccharides particularly suitable for terminal coupling into hybrids because of their particularly reactive chain termini (Westereng et al., 2016; Westereng et al., 2020). These enzymes produce lactones at the reducing end, which are more reactive towards amines than the masked aldehyde (Hernandez, Soliman, & Winnik, 2007; Zhang & Marchant, 1994; Ziegast & Pfannemuller, 1984) . Even more remarkable is the reported oxidation at C4 of the non-reducing ends of LPMO degraded cellulose (Isaksen et al., 2014) and hemicellulose (Agger et al., 2014). This opens an entirely novel and 'green' route for substitution at this position, marking the starting point for including cellulose in block polysaccharides of the ABA or ABC type (B being cellulose) or AB types where the cellulose can be either parallel or antiparallel to the A block.

In a recent article the reactivity of oxyamines and hydrazides at the NRE of periodate oxidised chitin oligomers was investigated (Mo, Schatz, & Christensen, 2021). In this case the oligomers were of the A_nM type obtained by degrading chitosans with excess nitric acid. It was confirmed by NMR that the M residue at the RE was as expected periodate resistant, whereas a reactive dialdehyde is formed at the NRE. Hence, both termini were reactive. This was taken one step further in reactions with sub-stoichiometric amounts of ADH and PDHA. This led to further polymerisation into longer chains of the type $(-A^*AAAM-PDHA-)_n$ (using a DP5 oligomer as example, A* denoting the C4-C4 dialdehyde). Interestingly, chains with DP larger than 30 were detected by aqueous SEC, meaning they were water-soluble, in contrast to chitins with the same DP. This opens for a wide range of new types of engineered and water-soluble polysaccharides containing repeating units of inherently water-insoluble oligosaccharides.

8. Example of block polysaccharide structures.

The coupling strategy based on ADH or PDHA has been successfully applied to design various block polysaccharide structures including symmetric block copolymers (A-*b*-A) and asymmetric ones (A-*b*-B). Chitin oligomers containing 4 residues of N-acetyl D-glucosamine (A unit) and a M unit at the reducing end were used to synthesize symmetric A_4M-ADH-MA_4 copolymer by simple mixing of equimolar amount of reduced A_4M-ADH conjugates and A_4M, resulting in a yield as high as 74% (Mo, Dalheim, et al., 2020). After subsequent reduction with PB, the relative yield was 83%. Unreacted A_4M oligomers were reduced and removed by gel filtration chromatography (GFC). Figure 7a shows the structure of the reduced A_4M-ADH-MA_4 and the ^{1}H-NMR spectrum after purification. From the side of asymmetric

copolymers, dextran oligomers of DP 6 obtained by hydrolysis of a parent sample and fractionated by GFC were coupled to reduced A_5M-ADH and A_5M-PDHA. The yields of A_5M-ADH-$Dext_6$ and A_5M-PDHA-$Dext_6$ were respectively 15% and 66% when using only one equivalent of $Dext_6$. Such relative low yields emphasize the limited availability of the aldehyde function at the reducing end of dextran compared to the permanent aldehyde end function (M unit) found in A_nM. The higher yield obtained with A_5M-PDHA is in line with the literature (Kwase et al., 2013). After reduction with PB, the yields reach satisfactory values of 85% for A_5M-ADH-$Dext_6$ and 92% for A_5M-PDHA-$Dext_6$. The structure and NMR spectra of the reduced and purified copolymers are given in Figure 7b-c.
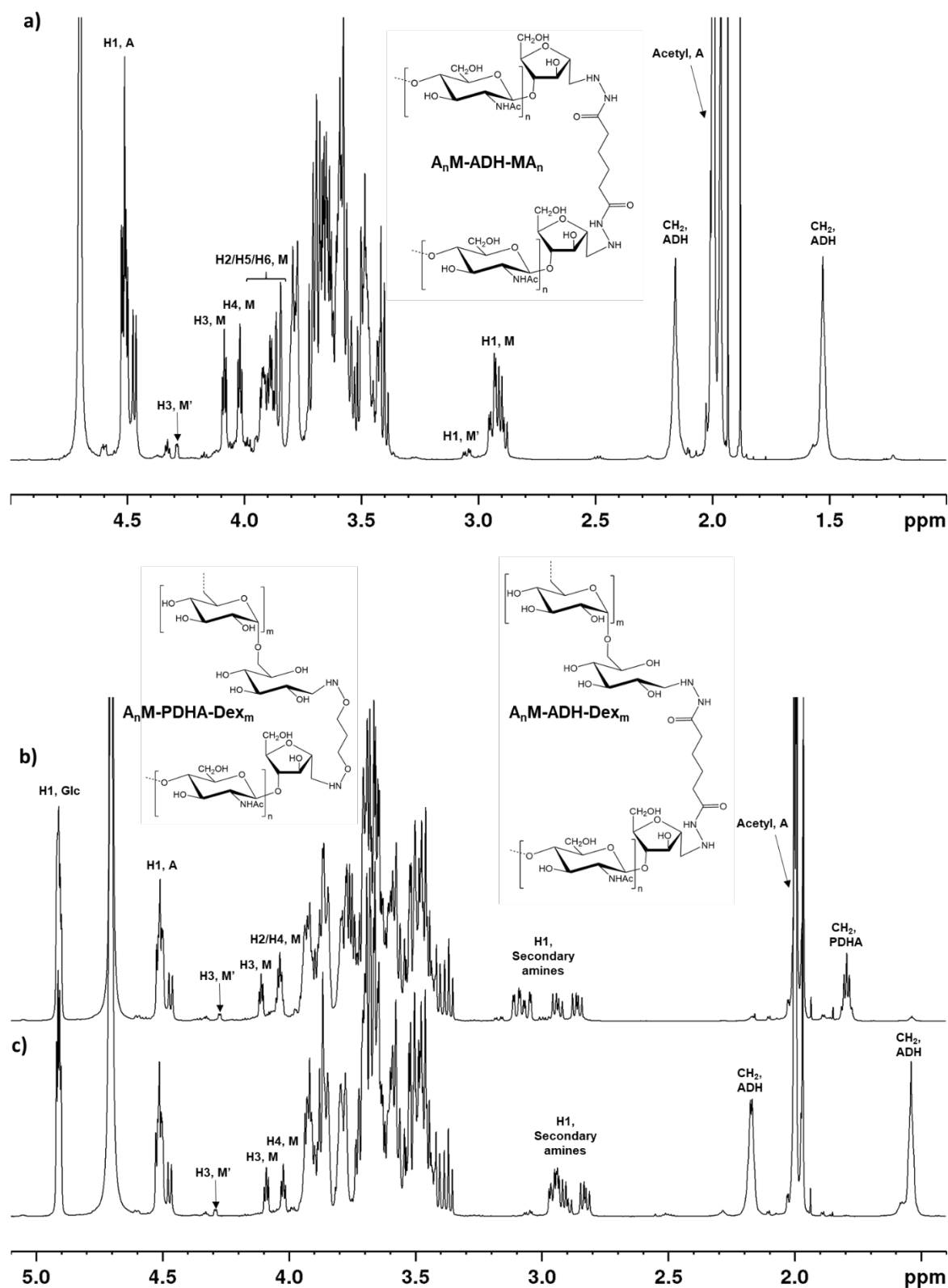
Fig. 7. Chemical structures and ^{1}H NMR spectra of various block polysaccharides obtained by the ADH/PDHA coupling approach after reduction of the hydrazone/oxime linkage and purification. a) A_4M-ADH-MA$_4$ where A is the N-acetyl D-glucosamine, b) A_5M-PDHA-Dex$_6$ and c) A_5M-ADH-Dex$_6$ where Dex is a dextran block. Adapted from (Mo, Dalheim, et al., 2020)

Alginate-based diblock polysaccharides have been also obtained (Solberg et al., 2021). First, the reactivity of the reducing end of oligoguluronate (G-blocks) and oligomannuronate (M-

blocks) with ADH and PDHA was studied. Briefly, much higher yields and reaction rates were obtained with PDHA whatever the nature of the alginate blocks. In this case, only E-/Z-oximes were formed. The reactivity observed with ADH is much lower with the predominant formation of β-*N*-pyranosides, in line with the conjugation of hydrazides and other reducing sugars. G-blocks were successfully coupled to various oligosaccharides blocks including dextran, β-1,3-glucan and chitin. As the reactivity of the reducing end of alginate is high, the coupling was performed by reacting native G-blocks with polysaccharide blocks end modified with PDHA. Figure 8a shows the chemical structure and SEC-MALS characterization of G_{12}-PDHA-Dex_{100}. The coupling was demonstrated by a significant shift in the elution volume of the purified block compared to the starting material.

Importantly, the Ca^{2+} induced self-assembly behaviour of the G-blocks is fully preserved in the copolymer structure. However, in contrast to most alginates, which upon introduction of Ca^{2+} form macroscopic hydrogels, or purified G-blocks, which precipitate, the diblocks formed small nanoparticles (Fig. 8b). A dialysis setup was used to slowly introduce Ca^{2+} and DLS was used to monitor the self-assembly at regular time intervals.
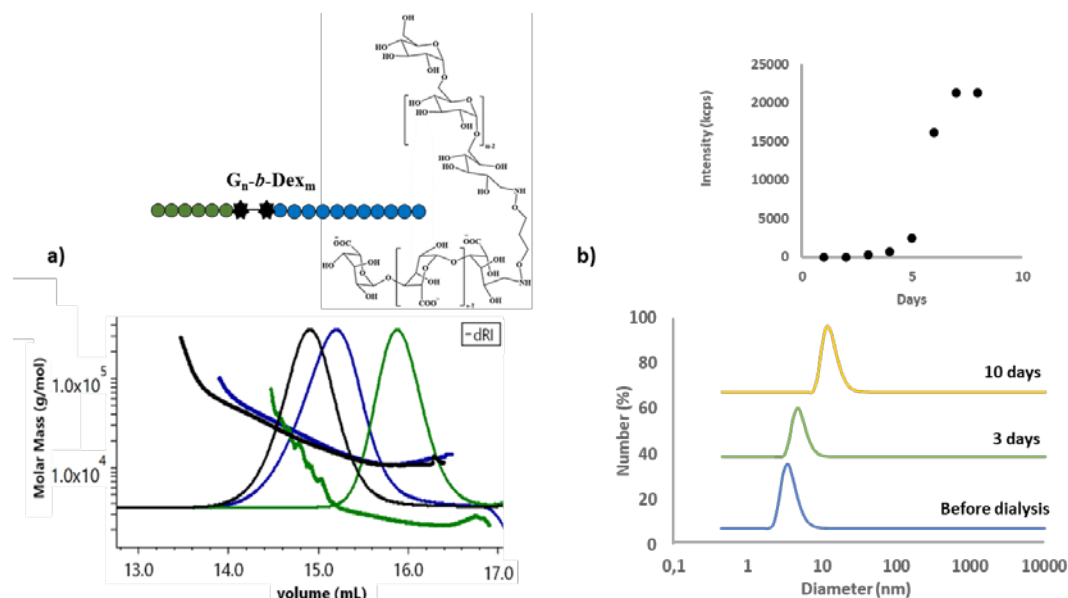

Fig. 8. a) A G_{12}-PDHA-Dex_{100} diblock was purified by GFC and analysed by SEC-MALS, the elution volume of the diblock (black) corresponded well with the coupling of Dex_{100}-PDHA (blue) and G_{12} (green). b) Self-assembly of G_{40}-PDHA-Dex_{100} into well-defined nanoparticles through dialysis against Ca^{2+} ions monitored by dynamic light scattering. The increase in the scattering intensity is shown (top right). Adapted from (Solberg et al., 2021).

Future and outlook

There is no doubt that block copolymers containing polysaccharides will be increasingly considered in the future because of their sustainability, biodegradability, and biological properties. A first achievement was performed in the late 2000s and early 2010s with the design of hybrid copolymer structures containing a polysaccharide block associated to a synthetic one. This coincided with the advent of the click chemistry based on the Huisgen 1,3-dipolar cycloaddition which has been widely applied to the copolymer field.

It seems now rather obvious that the next step would consist in developing copolymers exclusively made of polysaccharides, i.e. block polysaccharides. In this context, it seems appropriate to have a click chemistry which is specific of the reducing end of polysaccharides. Moreover, the general applicability of the chemistry will likely simplify effective incorporation of polysaccharides in biomacromolecules linearly.

Conclusions

Here, we have shown that difunctional linkers like ADH and PDHA based on hydrazide and oxyamine groups, respectively, are particularly suitable for click chemistry with polysaccharides. Moreover, they allow for the effective preparation of block polysaccharides. Advantages of these linkers include their very good reactivity with the reducing end at room temperature both in terms of yield and reaction rate, the absence of secondary reactions except for ADH for long reaction times, their water-solubility, the easy removal of excess product and the fact that they are both commercially available. Following the conjugation with the reducing end, the hydrazone (or oxime) can be stabilized by reduction in mild conditions with picoline borane or sodium cyanoborohydride. The synthesis of AB- or AA-type block copolymers is typically performed in only two steps, the activation of one block with ADH or PDHA followed by the coupling with the second block.

Among promising properties of diblock polysaccharides are the possibility to form stimuli-responsive core-corona nanoparticles as exemplified by the alginate-*b*-dextran/Ca^{2+} system.

More sophisticated structures can be obtained such as ABA copolymers based on a polysaccharide B block whose non-reducing end has been previously activated by a chemical or enzymatic approach to generate an aldehyde function. In a similar way we reported the formation of water-soluble multiblock polysaccharides of type (-A-PDHA-)$_n$ where A was a chitin oligomer being reactive at both termini.

To conclude, this simple PDHA/ADH-based chemistry offers several opportunities to design novel block polysaccharide structures with new properties.

References.

Agger, J. W., Isaksen, T., Varnai, A., Vidal-Melgosa, S., Willats, W. G. T., Ludwig, R., . . . Westereng, B. (2014). Discovery of LPMO activity on hemicelluloses shows the importance of oxidative processes in plant cell wall degradation. *Proceedings of the National Academy of Sciences,* 111(17), 6287-6292.

Baudendistel, O. R., Wieland, D. E., Schmidt, M. S., & Wittmann, V. (2016). Real-Time NMR Studies of Oxyamine Ligations of Reducing Carbohydrates under Equilibrium Conditions. *Chemistry-a European Journal,* 22(48), 17359-17365.

Belbekhouche, S., Ali, G., Dulong, V., Picton, L., & Le Cerf, D. (2011). Synthesis and characterization of thermosensitive and pH-sensitive block copolymers based on polyetheramine and pullulan with different length. *Carbohydrate Polymers,* 86(1), 304-312.

Bertozzi, C. R. (2011). A decade of bioorthogonal chemistry. *Accounts of Chemical Research,* 44(9), 651-653.

Bowman, K. A., Aarstad, O. A., Nakamura, M., Stokke, B. T., Skjåk-Bræk, G., & Round, A. N. (2016). Single molecule investigation of the onset and minimum size of the calcium-mediated junction zone in alginate. *Carbohydrate Polymers,* 148, 52-60.

Breitenbach, B. B., Schmid, I., & Wich, P. R. (2017). Amphiphilic Polysaccharide Block Copolymers for pH-Responsive Micellar Nanoparticles (vol 18, pg 2839, 2017). *Biomacromolecules,* 18(11), 3844-3845.

Chen, C., Wah Ng, D. Y., & Weil, T. (2020). Polymer bioconjugates: Modern design concepts toward precision hybrid materials. *Progress in Polymer Science*, 101241.

Christensen, B. E., & Smidsrød, O. (1996). Dependence of the content of unsubstituted (cellulosic) regions in prehydrolysed xanthans on the rate of hydrolysis by Trichoderma reesei endoglucanase. *International Journal of Biological Macromolecules,* 18(1-2), 93-99.

Cosenza, V. A., Navarro, D. A., & Stortz, C. A. (2011). Usage of alpha-picoline borane for the reductive amination of carbohydrates. *Archive for Organic Chemistry)*, 182-194.

Daus, S., Elschner, T., & Heinze, T. (2010). Towards unnatural xylan based polysaccharides: reductive amination as a tool to access highly engineered carbohydrates. *Cellulose,* 17(4), 825-833.

Derry, M. J., Fielding, L. A., & Armes, S. P. (2016). Polymerization-induced self-assembly of block copolymer nanoparticles via RAFT non-aqueous dispersion polymerization. *Progress in Polymer Science,* 52, 1-18.

Donati, I., & Paoletti, P. (2009). *Material properties of alginates*. In *Alginates: Biology and Applications*. Berlin, Heidelberg: Springer-Verlag

Draget, K. I., Moe, S. T., Skjåk-Bræk, G., & Smidsrød, O. (2006). *Alginates*. In A. M. Stephen, G. O. Phillips & P. A. Williams (Eds.), *Food Polysaccharides and Their Applications* (pp. 289-334). Boca Raton: CRC Press

Edwards, J. O., & Pearson, R. G. (1962). The Factors Determining Nucleophilic Reactivities. *Journal of the American Chemical Society,* 84(1), 16-24.

Espevik, T., Rokstad, A. M., Kulseng, B., Strand, B., & Skjåk-Bræk, G. (2009). *Mechanisms of the host immune response to alginate microcapsules*. In J.-P. Hallé, P. de Vos & L.

Rosenberg (Eds.), *The Bioartificial Pancreas and Other Biohybrid Therapies* (pp. 279-290): Research Science Post

Fuchs, K., Cardona Gloria, Y., Wolz, O. O., Herster, F., Sharma, L., Dillen, C. A., . . . Weber, A. N. (2018). The fungal ligand chitin directly binds TLR2 and triggers inflammation dependent on oligomer size. *EMBO Reports,* 19(12).

Goycoolea, F. M., Arguelles-Monal, W. M., Lizardi, J., Peniche, C., Heras, A., Galed, G., & Diaz, E. I. (2007). Temperature and pH-sensitive chitosan hydrogels: DSC, rheological and swelling evidence of a volume phase transition. *Polymer Bulletin,* 58(1), 225-234.

Gravdahl, M. (2021). Preparation, characterization, and solution properties of chitosan-b-dextran diblocks. (Vol. M. Sc.): NTNU - Norwegian University of Science and Technology.

Guibal, E., Touraud, E., & Roussy, J. (2005). Chitosan interactions with metal ions and dyes: Dissolved-state vs. solid-state application. *World Journal of Microbiology & Biotechnology,* 21(6-7), 913-920.

Hamley, I. W. (2009). Ordering in thin films of block copolymers: Fundamentals to potential applications. *Progress in Polymer Science,* 34(11), 1161-1210.

Haug, A., & Smidsrød, O. (1965). The effect of divalent metals on the properties of alginate solutions. II. Comparison of different metal ions. *Acta Chemica Scandinavica,* 19, 341-351.

Hayakawa, D., Nishiyama, Y., Mazeau, K., & Ueda, K. (2017). Evaluation of hydrogen bond networks in cellulose Ibeta and II crystals using density functional theory and Car-Parrinello molecular dynamics. *Carbohydrate Research,* 449, 103-113.

Heise, K., Delepierre, G., King, A. W. T., Kostiainen, M. A., Zoppe, J., Weder, C., & Kontturi, E. (2021). Chemical Modification of Reducing End-Groups in Cellulose Nanocrystals. *Angewandte Chemie-International Edition,* 60(1), 66-87.

Hernandez, O. S., Soliman, G. M., & Winnik, F. M. (2007). Synthesis, reactivity, and pH-responsive assembly of new double hydrophilic block copolymers of carboxymethyldextran and poly(ethylene glycol). *Polymer,* 48(4), 921-930.

Hirano, S., & Yagi, Y. (1981). Periodate-Oxidation of the Non-Reducing End-Groups of Substrates Increases the Rates of Enzymic Hydrolyses by Chitinase and by Lysozyme. *Carbohydrate Research,* 92(2), 319-322.

Horn, S. J., Sørbotten, A., Synstad, B., Sikorski, P., Sørlie, M., Vårum, K. M., & Eijsink, V. G. (2006). Endo/exo mechanism and processivity of family 18 chitinases produced by Serratia marcescens. *FEBS Journal,* 273(3), 491-503.

Imai, T., Watanabe, T., Yui, T., & Sugiyama, J. (2002). Directional degradation of beta-chitin by chitinase A1 revealed by a novel reducing end labelling technique. *FEBS Letters,* 510(3), 201-205.

Isaksen, T., Westereng, B., Aachmann, F. L., Agger, J. W., Kracher, D., Kittl, R., . . . Horn, S. J. (2014). A C4-oxidizing lytic polysaccharide monooxygenase cleaving both cellulose and cello-oligosaccharides. *Journal of Biololgical Chemistry,* 289(5), 2632-2642.

Jo, I. S., Lee, S., Zhu, J. T., Shim, T. S., & Yi, G. R. (2017). Soft patchy micelles. *Current Opinion in Colloid & Interface Science,* 30, 97-105.

Kataoka, K., Harada, A., & Nagasaki, Y. (2012). Block copolymer micelles for drug delivery: Design, characterization and biological significance. *Advanced Drug Delivery Reviews,* 64, 37-48.

Kwase, Y. A., Cochran, M., & Nitz, M. (2013). *Protecting-Group-Free Glycoconjugate Synthesis: Hydrazide and Oxyamine Derivatives in N-Glycoside Formation.* In D. B.

Werz & S. Vidal (Eds.), *Modern synthetic methods in carbohydrate chemistry: From monosaccharides to complex glycoconjugates* (pp. 67-96): Wiley

Lallana, E., Fernandez-Megia, E., & Riguera, R. (2009). Surpassing the Use of Copper in the Click Functionalization of Polymeric Nanostructures: A Strain-Promoted Approach. *Journal of the American Chemical Society,* 131(16), 5748-5750.

Lobling, T. I., Borisov, O., Haataja, J. S., Ikkala, O., Groschel, A. H., & Muller, A. H. E. (2016). Rational design of ABC triblock terpolymer solution nanostructures with controlled patch morphology. *Nature Communications,* 7.

Lohmann, J., Houga, C., Driguez, H., Wilson, J., Destarac, M., Fort, S., . . . Gnanou, Y. (2009). Hybrid Block Copolymers Incorporating Oligosasaccharides and D Synthetic Blocks Grown by Controlled Radical Polymerization. *Controlled/Living Radical Polymerization: Progress in Atrp,* 1023, 231-240.

Mai, Y. Y., & Eisenberg, A. (2012). Self-assembly of block copolymers. *Chemical Society Reviews,* 41(18), 5969-5985.

Mergy, J., Fournier, A., Hachet, E., & Auzely-Velty, R. (2012). Modification of polysaccharides via thiol-ene chemistry: A versatile route to functional biomaterials. *Journal of Polymer Science Part a-Polymer Chemistry,* 50(19), 4019-4028.

Mo, I. V., Dalheim, M. Ø., Aachmann, F. L., Schatz, C., & Christensen, B. E. (2020). 2,5-Anhydro D mannose end-functionalised chitin oligomers activated by dioxyamines or dihydrazides as precursors of diblock oligosaccharides *Biomacromolecules,* 21, 2884-2895

Mo, I. V., Feng, Y., Dalheim, M. Ø., Solberg, A., Aachmann, F. L., Schatz, C., & Christensen, B. E. (2020). Activation of enzymatically produced chitooligosaccharides by dioxyamines and dihydrazides. *Carbohydrate Polymers,* 232.

Mo, I. V., Schatz, C., & Christensen, B. E. (2021). Functionalisation of the non-reducing end of chitin by selective periodate oxidation: A new approach to form complex block polysaccharides and water-soluble chitin-based block polymers. *Carbohydrate Polymers,* 261, 118193.

Montembault, A., Viton, C., & Domard, A. (2005a). Physico-chemical studies of the gelation of chitosan in a hydroalcoholic medium. *Biomaterials,* 26(8), 933-943.

Montembault, A., Viton, C., & Domard, A. (2005b). Rheometric study of the gelation of chitosan in aqueous solution without cross-linking agent. *Biomacromolecules,* 6(2), 653-662.

Moussa, A., Crepet, A., Ladaviere, C., & Trombotto, S. (2019). Reducing-end "clickable" functionalizations of chitosan oligomers for the synthesis of chitosan-based diblock copolymers. *Carbohydrate Polymers,* 219, 387-394.

Novoa-Carballal, R., & Muller, A. H. E. (2012). Synthesis of polysaccharide-b-PEG block copolymers by oxime click. *Chemical Communications,* 48(31), 3781-3783.

Okuyama, K., Noguchi, K., Miyazawa, T., Yui, T., & Ogawa, K. (1997). Molecular and Crystal Structure of Hydrated Chitosan. *Macromolecules,* 30(19), 5849-5855.

Oprea, M., & Voicu, S. I. (2020). Recent advances in composites based on cellulose derivatives for biomedical applications. *Carbohydrate Polymers,* 247.

Otsuka, I., Osaka, M., Sakai, Y., Travelet, C., Putaux, J. L., & Borsali, R. (2013). Self-assembly of maltoheptaose-block-polystyrene into micellar nanoparticles and encapsulation of gold nanoparticles. *Langmuir,* 29(49), 15224-15230.

Pickenhahn, V. D., Darras, V., Dziopa, F., Biniecki, K., De Crescenzo, G., Lavertu, M., & Buschmann, M. D. (2015). Regioselective thioacetylation of chitosan end-groups for nanoparticle gene delivery systems. *Chemical Science,* 6(8), 4650-4664.

Ruzette, A. V., & Leibler, L. (2005). Block copolymers in tomorrow's plastics. *Nature Materials,* 4(1), 19-31.

Schacher, F. H., Rupar, P. A., & Manners, I. (2012). Functional Block Copolymers: Nanostructured Materials with Emerging Applications. *Angewandte Chemie-International Edition,* 51(32), 7898-7921.

Schatz, C., & Lecommandoux, S. (2010). Polysaccharide-Containing Block Copolymers: Synthesis, Properties and Applications of an Emerging Family of Glycoconjugates. *Macromol Rapid Commun,* 31(19), 1664-1684.

Sikorski, P., Hori, R., & Wada, M. (2009). Revisit of alpha-chitin crystal structure using high resolution X-ray diffraction data. *Biomacromolecules,* 10(5), 1100-1105.

Sikorski, P., Mo, F., Skjåk-Bræk, G., & Stokke, B. T. (2007). Evidence for egg-box-compatible interactions in calcium-alginate gels from fiber X-ray diffraction. *Biomacromolecules,* 8(7), 2098-2103.

Sjöström, E. (1993). *Wood Chemistry*: Academic Press.

Sletmoen, M., & Stokke, B. T. (2008). Review : Higher order structure of (1,3)-beta-D-glucans and its influence on their biological activities and complexation abilities. *Biopolymers,* 89(4), 310-321.

Sletten, E. M., & Bertozzi, C. R. (2009). Bioorthogonal Chemistry: Fishing for Selectivity in a Sea of Functionality. *Angewandte Chemie International Edition,* 48(38), 6974-6998.

Solberg, A. (2017). Hydrazide Conjugated Oligoguluronates. (Vol. M.Sc.): NTNU-Norwegian University of Science and Technology.

Solberg, A., Mo, I. V., Aachmann, F. L., Schatz, C., & Christensen, B. E. (2021). Alginate-based diblock polymers: Preparation, characterisation, and Ca-induced self-assembly. *Polymer Chemistry,* 12(38), 5393-5558.

Suzuki, S., Christensen, B. E., & Kitamura, S. (2011). Effect of mannuronate content and molecular weight of alginates on intestinal immunological activity through Peyer's patch cells of C3H/HeJ mice. *Carbohydrate Polymers* 83, 629–634.

Tomofuji, Y., Yoshiba, K., Christensen, B. E., & Terao, K. (2019). Single-chain conformation of carboxylated schizophyllan, a triple helical polysaccharide, in dilute alkaline aqueous solution. *Polymer Gels and Networks,* 185, 121944.

Upadhyay, K. K., Le Meins, J. F., Misra, A., Voisin, P., Bouchaud, V., Ibarboure, E., . . . Lecommandoux, S. (2009). Biomimetic Doxorubicin Loaded Polymersomes from Hyaluronan-block-Poly(gamma-benzyl glutamate) Copolymers. *Biomacromolecules,* 10(10), 2802-2808.

van Zoelen, W., Buss, H. G., Ellebracht, N. C., Lynd, N. A., Fischer, D. A., Finlay, J., . . . Segalman, R. A. (2014). Sequence of Hydrophobic and Hydrophilic Residues in Amphiphilic Polymer Coatings Affects Surface Structure and Marine Antifouling/Fouling Release Properties. *ACS Macro Letters,* 3(4), 364-368.

Vaaje-Kolstad, G., Westereng, B., Horn, S. J., Liu, Z., Zhai, H., Sorlie, M., & Eijsink, V. G. (2010). An oxidative enzyme boosting the enzymatic conversion of recalcitrant polysaccharides. *Science,* 330(6001), 219-222.

Wang, Z., Shi, C., Wu, X., & Chen, Y. (2014). Efficient access to the non-reducing end of low molecular weight heparin for fluorescent labeling. *Chemical Communications,* 50(53), 7004-7006.

Westereng, B., Arntzen, M. O., Aachmann, F. L., Varnai, A., Eijsink, V. G. H., & Agger, J. W. (2016). Simultaneous analysis of C1 and C4 oxidized oligosaccharides, the products of lytic polysaccharide monooxygenases acting on cellulose. *Journal of Chromatography A,* 1445, 46-54.

Westereng, B., Kracun, S. K., Leivers, S., Arntzen, M. O., Aachmann, F. L., & Eijsink, V. G. H. (2020). Synthesis of glycoconjugates utilizing the regioselectivity of a lytic polysaccharide monooxygenase. *Scientific Reports,* 10(1), 13197.

Wu, D. J., Zhu, L. X., Li, Y., Zhang, X. L., Xu, S. M., Yang, G. S., & Delair, T. (2020). Chitosan-based Colloidal Polyelectrolyte Complexes for Drug Delivery: A Review. *Carbohydrate Polymers,* 238.

Zhang, T., & Marchant, R. E. (1994). Novel Polysaccharide Surfactants: Synthesis of Model Compounds and Dextran-Based Surfactants. *Macromolecules,* 27(25), 7302-7308.

Ziegast, G., & Pfannemuller, B. (1984). Linear and Star-Shaped Hybrid Polymers .2. Coupling of Monosaccharide and Oligosaccharide to Alpha,Omega-Diamino Substituted Poly(Oxyethylene) and Multifunctional Amines by Amide Linkage. *Macromolecular Rapid Communications,* 5(7), 373-379.

Supporting Information

Click chemistry for block polysaccharides with dihydrazide and dioxyamine linkers - a review

Amalie Solberg,[a] Ingrid V. Mo,[a] Line Aa. Omtvedt,[a] Berit L. Strand,[a] Finn L. Aachmann,[a] Christophe Schatz,*[b] and Bjørn E. Christensen*[a]

[a] NOBIPOL, Department of Biotechnology and Food Science, NTNU Norwegian University of Science and Technology, Sem Sælands vei 6/8, NO-7491 Trondheim, Norway

[b] LCPO, Université de Bordeaux, UMR 5629, ENSCBP, 16, Avenue Pey Berland, 33607 Pessac Cedex, France

Contents

Preparation of alginate-*b*-cyclodextrins blocks using Cu(I)-catalyzed azide-alkyne cycloaddition

Results

Alkyne hydrazide (5-hexyne-1-hydrazide) was conjugated to the reducing end of G_n-, M_n- and polyalternating $(MG)_m$-oligomers using methods adapted from the previously described protocol for hydrazides with alginates (Solberg, Mo et al. 2021), providing conjugates functionalized with a terminal alkyne group. Subscript n denotes the number of residues per chain. In the case of polyalternating $(MG)_m$, m denotes the number of MG-residues. The ^{1}H-NMR spectra are shown in Figs. S1 a-c.
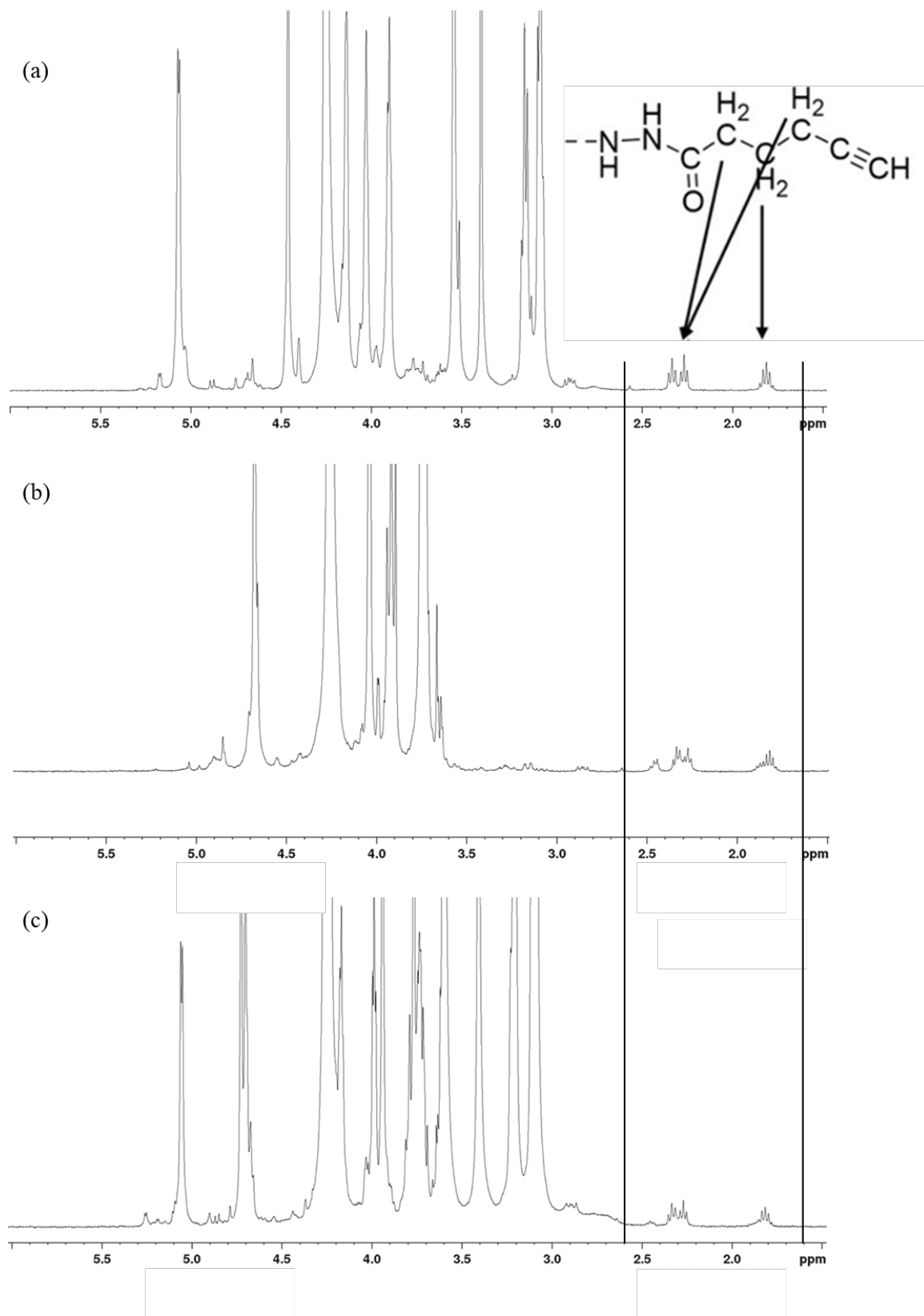
Figure S1: ^{1}H-NMR (400 MHz, 83°C) spectra of a) G_{14-15}, b) M_{14} and c) polyalternating $(MG)_7$ terminally conjugated to alkyne hydrazide.

The alkyne functionalized oligomers were subsequently clicked to azide functionalized cyclodextrins (β- or γ-N_3-CyDs) using copper(I)-catalyzed azide-alkyne cycloaddition (CuAAC) (Omtvedt, Dalheim et al. 2019). The formation of M_n-*b*-CyD and $(MG)_m$-*b*-CyD was demonstrated by the characteristic triazole signal at 7.8 ppm in the ^{1}H-NMR spectra. The ^{1}H-NMR spectra of M_n-*b*-βCyD and M_n-*b*-γCyD are shown in Fig. S2. The ^{1}H-NMR spectra of $(MG)_m$-*b*-βCyD and $(MG)_m$-*b*-γCyD are given in Fig. S3. However, the click reaction to CD was unsuccessful in the case of oligoguluronates (G_n). No triazole signals were observed (Fig. S4).
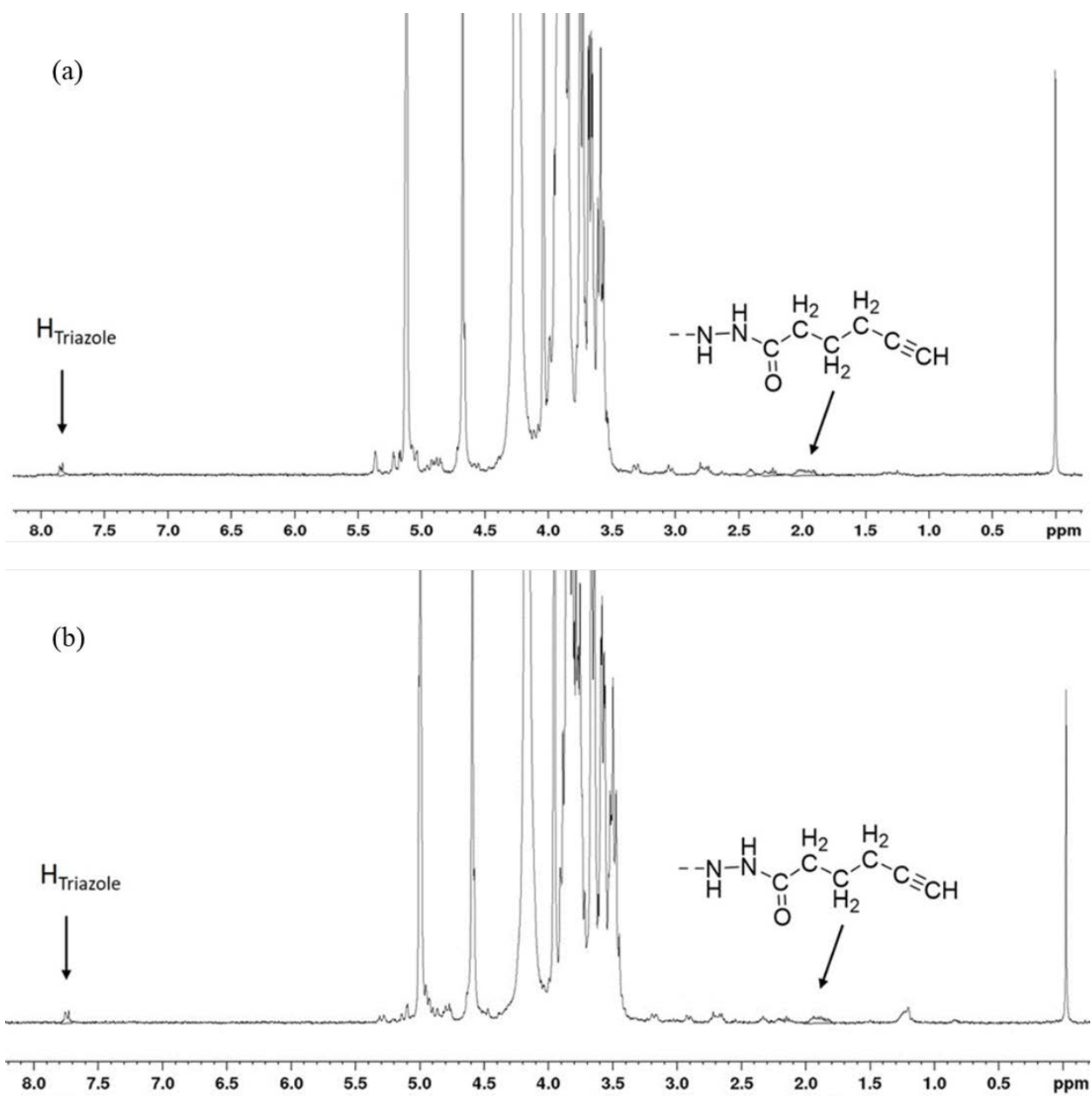
Figure S2: ^{1}H-NMR spectra (400 MHz, 83°C) of alkyne functionalized M-oligomer (M[14]) grafted with a) γ-CyD and b) β-CyD using CuAAC.

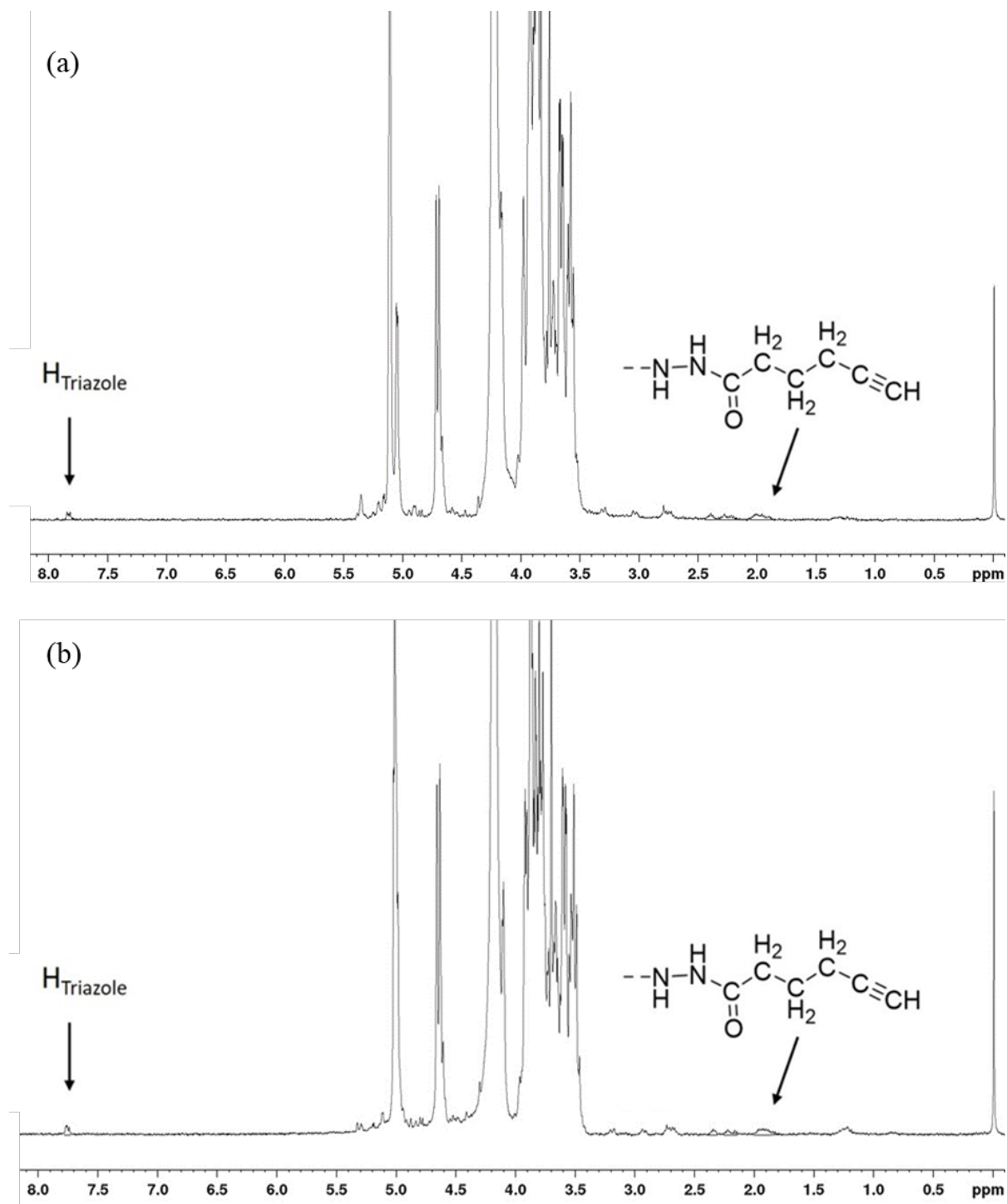**Figure S3**: ^{1}H-NMR spectra (400 MHz, 83°C) of alkyne functionalized polyalternating (MG)$_7$-oligomer grafted with a) γ-CyD and b) β-CyD using CuAAC.
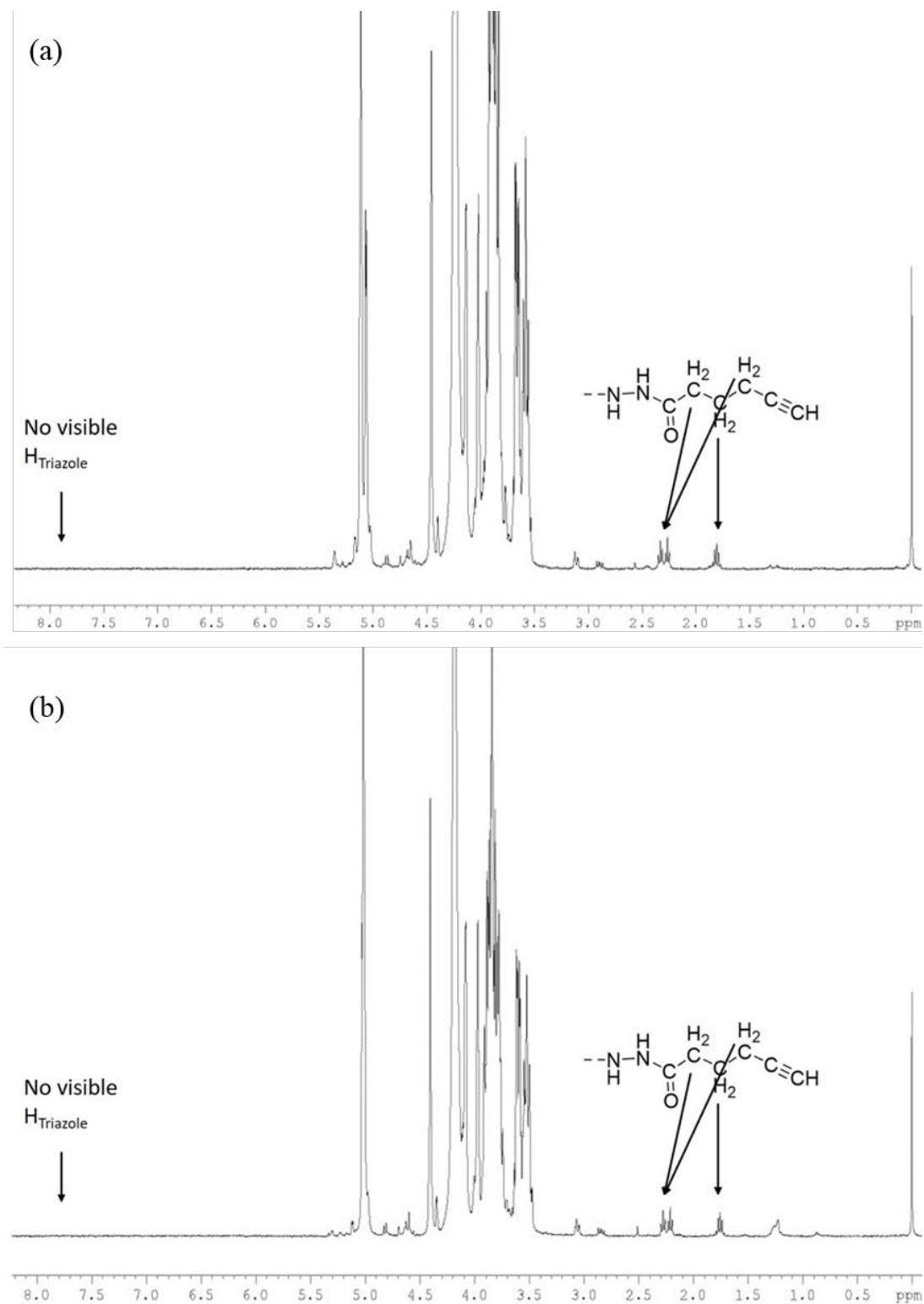
Figure S4: ^{1}H-NMR spectra (400 MHz, 83°C) of azide functionalized G$_{14}$-oligomers (G$_{14}$-*b*-N$_3$) after reaction with a) γ-CyD or b) β-CyD using CuAAC. The absence of triazole signals show that the click reaction did not occur.

Preparation of oligoguluronate-*b*-peptide blocks using Cu-free strain-promoted azide-alkyne cycloaddition

Strain-promoted azide alkyne cycloaddition (SPAAC) can be performed in the absence of metal catalyst. The approach was therefore investigated for the preparation of oligoguluronate-containing block structures. As a first step, aminooxy-PEG-spacers containing a reactive azide terminus (N_2OCH_2-PEG_5-N_3) was used to conjugate to oligoguluronates having DP_n 25. The conjugates were reduced by α-picoline borane and purified by GFC (Fig. S5).
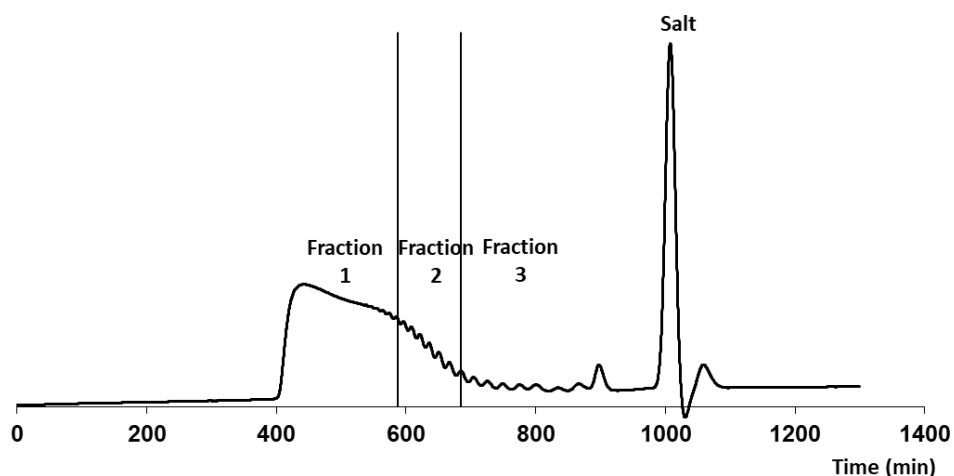

Figure S5: GFC chromatograms of the reaction mixture (200 mg) with oligoguluronate (DP_n 25) reacted with aminooxy-PEG_5-N_3 (2 equiv.) with reduction (6 equiv. PB) (500 mM NaAc-buffer pH 4).

In the next step SPAAC was utilized to add the peptide (1.2 molar excess) using the terminal cyclooctyne peptide derivative (DBCO-GRGDSP). The block was purified by GFC and subsequently characterized by ^{1}H-NMR, DOSY and SEC-MALS with an in-line viscosity detector. The results are shown in Fig. S6 and Table S1.

Table S1: Molar mass averages of a guluronate-PEG-N_3 clicked to a DBCO-functionalized peptide (DBCO-GRGDSP) to form a G_n-*b*-peptide block. The starting materials are included for comparison. The data were obtained from SEC-MALS with an in-line viscosity detector.

Sample	M_w (kDa)	[n] (mL/g)
G_n-PEG_5-N_3	6.8	22.8
DBCO-peptide	1.1	3.3
G_n-*b*-peptide	7.9	23.1
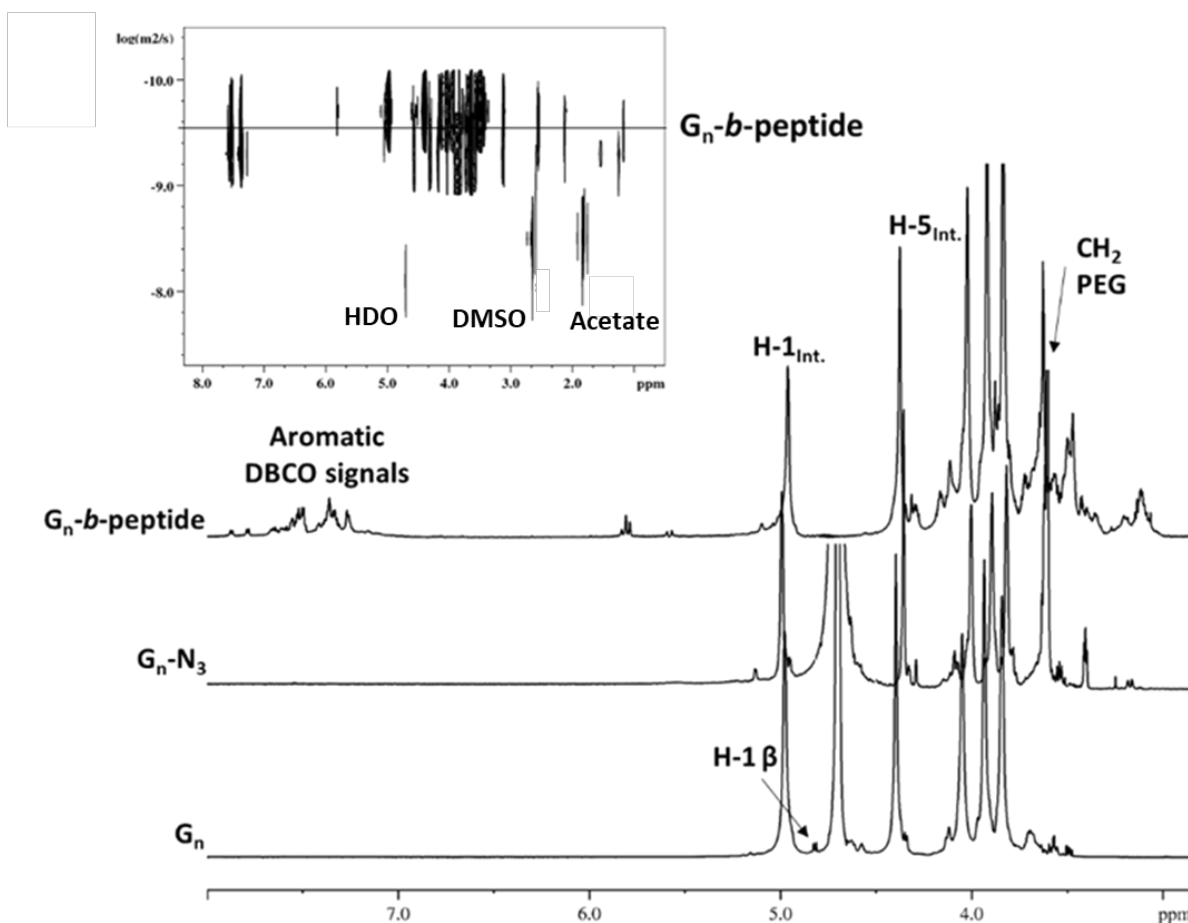
Figure S6: Stack of ^{1}H-NMR spectra of guluronate DP_n 34 (G_{34}), G_{34}-*b*-N_3 (600 MHz, 27°C) and G_{34}-*b*-peptide (the two latter were purified by SEC prior to analyses) (800 MHz, 25°C). A DOSY (800MHz, 25°C) of the G_{34}-*b*-peptide block (after purfification) is included.

The same approach was used for the preparation of fluorescently labelled guluronate (DP_n 28, disperse (not fractionated)). Here, stochiometric amounts (1:1) of a DBCO-functionalized fluorescent probe (Alexa488) was clicked to G_n-*b* - N_3. The azide functionalized guluronate (G_{29}-N_2OCH_2-PEG5-N_3) and G_{29}-b-Alexa488 were analysed by ^{1}H-NMR and DOSY, Fig. S7.
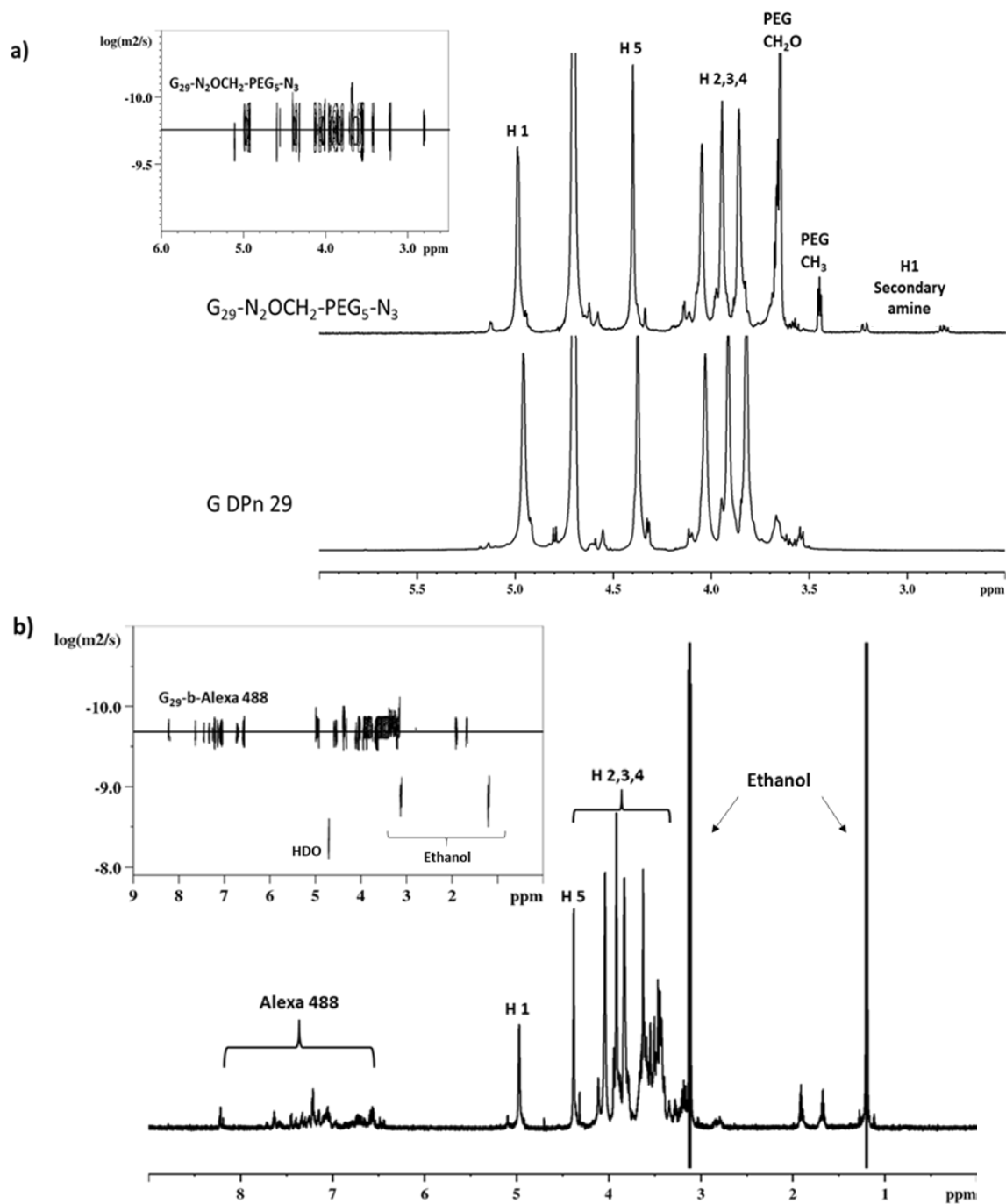
Figure S7: ^{1}H-NMR spectra (600 MHz, 2) and DOSY (upper left) of a) guluronate DP$_n$ 29 (G$_{29}$) terminally conjugated to aminoox-PEG$_5$-N$_3$ (G$_{29}$-N$_2$OCH$_2$-PEG$_5$-N$_3$) (with reduction by α-picoline borane, after purification by GFC and dialysis) and b) G$_{29}$-b-Alexa488 in D$_2$O (800 MHz, 25°C). The figure is reprinted from Brativnyk, A (Brativnyk 2020).

References

Brativnyk, A. (2020). Terminally modified alginates as universal tool for its bi-functionalization. (Vol. M. Sc.): NTNU-Norwegian University of Science and Technology.

Omtvedt, L. A., Dalheim, M. Ø., Nielsen, T.T., Larsen, K. L., Strand, B. L., and Aachmann, F. L. (2019). Efficient grafting of cyclodextrin to alginate and performance of the hydrogel for release of model drug. *Scientific reports* **9**(1): 1-11.

Solberg, A., Mo, I. V., Aachmann, F. L., Schatz, C., & Christensen, B. E. (2021). Alginate-based diblock polymers: Preparation, characterisation, and Ca-induced self-assembly. *Polymer Chemistry.* In press (Accepted 7 Sept. 2021).